TECHNISCHE
UNIVERSITÄT
WIEN

DIPLOMARBEIT

Core-Shell particles toughening of photopolymers used in additive manufacturing

ausgeführt zum Zwecke der Erlangung des akademischen Grades
eines Diplom-Ingenieurs unter der Leistung von

Ao.Univ.Prof. Dipl.-Ing. Dr.mont. Jürgen Stampfl
Projektass. Dipl.-Ing. Dr.techn. Peter Dorfinger
E308
Institut für Werkstoffwissenschaften und Werkstofftechnologie
Bereich Nichtmetallische Werkstoffe

Eingereicht an der Technischen Universität Wien
Fakultät für Maschinenwesen und Betriebswissenschaften
von

Alexandre Mégret

Matrikelnummer: 1528268
Sonnenallee 41/S517B, 1220 Wien

Wien, im Juni 2017

Unterschrift

Acknowledgements

First I would like to thank my supervisors Prof. Jürgen Stampfl and Dr. Peter Dorfinger for their help to find the right path during my thesis. A great thanks to Peter which has explained me the printer operations and has always answered all my questions.

I would also thank all the people of the group working on *functional non-metals* from *Institut für Werkstoffwissenschaft und Werkstofftechnologie* at TU Wien, which have given me a very good welcome. Concerning the experiments, I would like to thank Stefan Zellhofer and Gerhard Kern for their availability in the DMA-measurements as well as Thomas Koch for the tensile tests.

Finally, I would like to thank my family (especially my father which has read and has given me his feedback on my work) and of course all my friends during these two years T.I.M.E. exchange at TU Wien.

Contents

Kurzfassung

Heute haben die additiven Fertigungsverfahren in der Industrie eine große Bedeutung. Sie sind schnelle Technologien, mit denen auch, gegenüber von traditionellen Fertigungsverfahren, ganz neue Geometrie hergestellt werden können. Aufgrund der hohen Genauigkeit der hergestellten Objekte werden sie in vielen verschiedenen Branchen wie Luft- und Raumfahrt, Medizin eingesetzt.

Polymere werden für ihre besonderen Eigenschaften immer häufiger benutzt. Ihr geringes Gewicht (versus Metalle oder Keramiken) ist ein Vorteil. Polymere werden in verschiedenen Bereichen verwendet, um Gewicht der Strukturen zu sparen. Es ist daher wichtig, die mechanischen Eigenschaften von Polymeren und Photopolymeren zu verbessern. In dieser Arbeit wird ein bestimmter Typ des Schlagzähmodifizierers verwendet, die sogenannten *Core-Shell-Particles*. Artikel [1] sagt, dass Kautschukteilchen die mechanischen Eigenschaften von Polymeren verbessern können: ab einem gewissen Gehalt von *Core-Shell-Particles* kann die Schlagzähigkeit von Epoxiharzen maßgeblich verbessert werden.

In dieser Diplomarbeit werden Photopolymere mittels Stereolithographie hergestellt. Dieses additive Fertigungsverfahren benutzt ein Laser im UV-Bereich, um die Harzen zu polymerisieren. Das Ziel dieser Arbeit ist die mechanischen Eigenschaften zu verbessern, ohne die thermischen Eigenschaften zu verlieren. Das ideale Material hat eine hohe Bruchdehnung, einen hohe Schlagfestigkeit und einen Speichermodul, welcher mehr oder weniger konstant ist über einen großen Temperaturbereich.

Introduction

Nowadays additive manufacturing has taken a huge importance in industry. There are fast technologies used to build various objects with more or less all shapes possible. Due to the high accuracy of the manufactured objects, they are used in lots of different industries like aerospace, medicine where precision is needed. Moreover, those technologies allow rapid prototyping, which is a quick way to design new and innovative materials.

Polymers are also more and more often used in industries due to their particular properties. They have different mechanical properties than metals or ceramics but their low weight is an advantage. In different areas, polymer is used to save weight of structures, thus its demand has increased a lot. It is thus important to improve mechanical properties of polymers. In this thesis, a particular type of impact modifier, the so-called *core-shell particles* will be used. Article [1] says that rubber particles are able to improve mechanical properties: at constant particle size, impact strength versus rubber content curves exhibit a step at a precise rubber content (see figure 1).

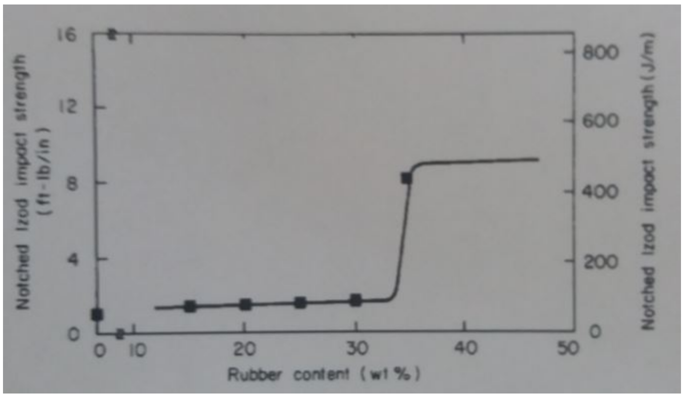

Figure 1 – Izod impact strength as function of rubber content [1]

In this thesis, photopolymers will be manufactured by stereolithography. It is a kind of additive manufacturing using a laser in UV-range to polymerize resins. As said before, the goal of this thesis is to improve mechanical properties without losing thermal properties. The ideal material would have high elongation at break and high impact strength while its storage modulus remains more or less constant in the temperature range of its application.

The first chapter of this thesis is the background where additive manufacturing technologies, photopolymers, toughening mechanisms and technical polymers will be explained in detail. The second chapter is the method which contains all information on the preparation of the formulations, the parameters of the printing, the post-curing and the different tests. The last chapter is dealing with the results.

Chapter 1

Background

1.1 Additive manufacturing technologies (AMT)

Additive manufacturing contains all technologies of fabrication of objects by joining material, in opposition to subtractive processes (machining, for example, where generally matter is taken out) or consolidation processes (casting, moulding). Technologies directly build objects from 3D digital models and it is usually done layer by layer. Additive manufacturing allows rapid prototyping of objects. It is rigorously defined in the Standard Terminology [2] as *the process of joining materials to make objects from 3D model data, usually layer upon layer, as opposed to subtractive manufacturing methodologies.*

1.1.1 Technologies

Additive manufacturing includes lots of processes [3], [4], [5] which are divided into different categories as described in figure 1.1: **vat photopolymerization processes** (stereolithography), **material jetting processes** (Inkjet), **powder bed fusion processes** (selective laser sintering/melting), **directed energy deposition processes** (electron beam melting), **binder jetting processes** (powder-binder bonding), **material extrusion processes** (fused deposition modelling), **sheet lamination processes** (laminated object manufacturing), ...

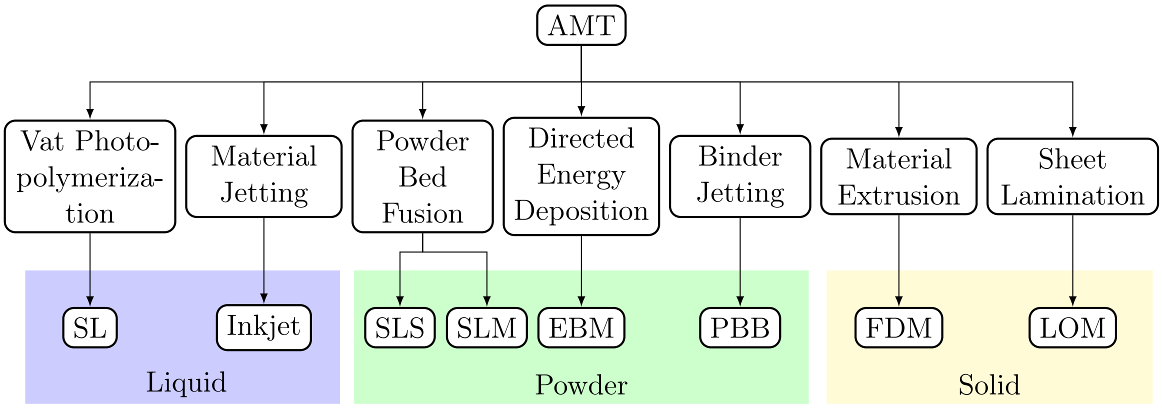

Figure 1.1 – Overview of additive manufacturing technologies [2]

The primary materials are resins, plastics, metals, ceramics and can be in the form of powder, liquid or solid. The major advantages of these processes are the manufacturing speed, the ability to build complex shapes, the possibility to share the 3D-files, the rationale use of material with reduced waste (near-net-shape technologies), and the possibility of building multi-material objects. However, for high quantities of objects or large parts, it is better to use conventional technologies.

Stereolithography (SL)

Stereolithography is a liquid-based process in which curing or solidification of a photosensitive resin occurs. A laser in the UV-range is usually used. The basic of this process is the photopolymerization (with help of a photoinitiator, a liquid monomer is converted into a solidified polymer by applying UV light). The machine contains a building platform, on which the objects are built, a material vat where the liquid monomers are stored and a laser which will scan layers. This laser usually works with a low-power and with focused beam. The process is represented in figure 1.2.

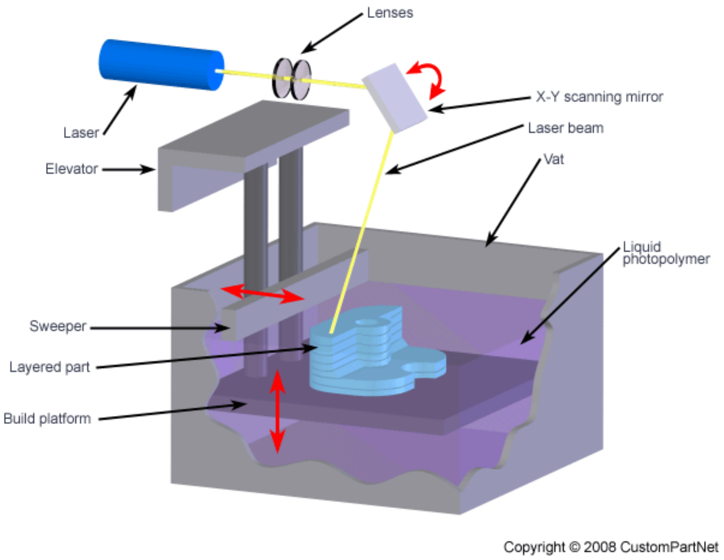

Copyright © 2008 CustomPartNet

Figure 1.2 – Sketch of stereolithography [6]

Jetting systems (Inkjet)

Jetting systems are liquid-based processes where a photosensitive monomer is applied on the building platform through nozzles print heads. These nozzles move in xy plane and draw each layer. The building platform is placed into a chamber containing an UV lamp which is switched on at the end of each layer. This lamp cures each layer one by one. Figure 1.3 represents this technology. This technology is based on 2D printing.

Selective Laser Sintering (SLS) and Selective Laser Melting (SLM)

Selective Laser Sintering/Melting is a powder-based process where a CO_2 laser is used to fuse fine powder into layers (figure 1.4). The laser beam draws the contour of each layer directly coming from the CAD-file and material is sintered/molten when the laser beam touches it. The building process usually takes place in a nitrogen filled chamber to avoid oxidation of the powder and thus this degradation. Temperature is chosen just below the melting point or the glass transition temperature of the powder. The advantages of these techniques is that objects can be manufactured with a wide range of material (polymers, metals, ceramics) and that powder can be recycled.

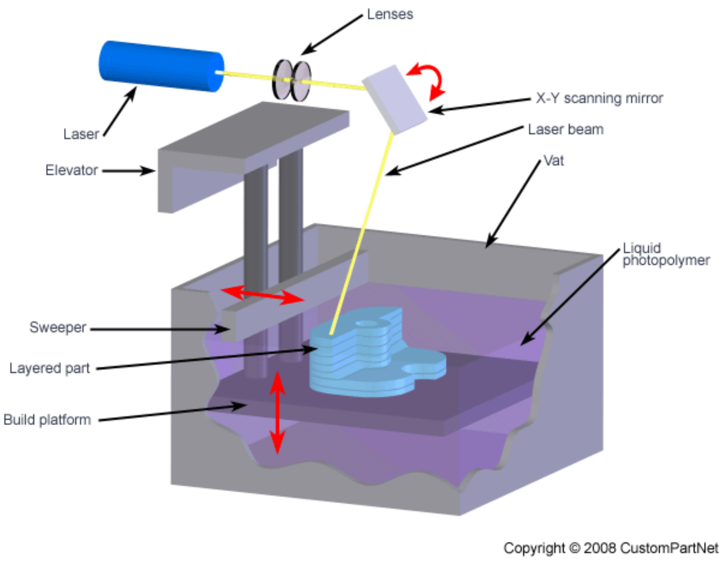

Figure 1.3 – Sketch of Inkjet [6]

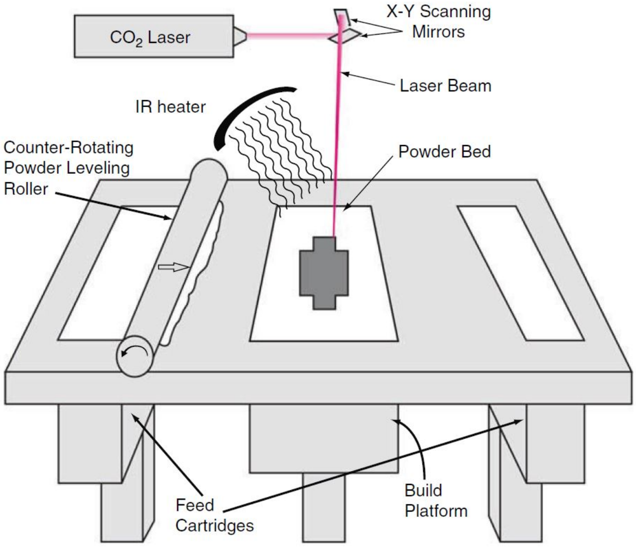

Figure 1.4 – Sketch of the selective laser sintering [3]

Electron Beam Melting (EBM)

Electron Beam Melting is a powder-based process in which a high-energy electron beam is used to fuse metallic powder under vacuum conditions. The electron beam is focused on the surface and scans layers in xy-directions. As the electron beam has a high energy, it goes deeper in the material and thus the scanning speed can be increased. Figure 1.5 represents this process.

Powder-bond Binding (PBB)

Powder-bond binding is a 3D-printing powder-based technique in which the powder particles are bounded together with a liquid binder. This liquid binder is injected on the top of the powder bed. Figure 1.6 represents this process. Two different companies have developed this technology: Z-Corporation and Ex-One LLC's Prometal Division [4].

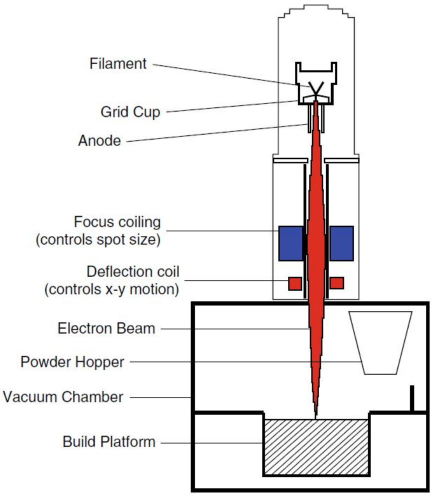

Figure 1.5 – Sketch of the electron beam melting [3]

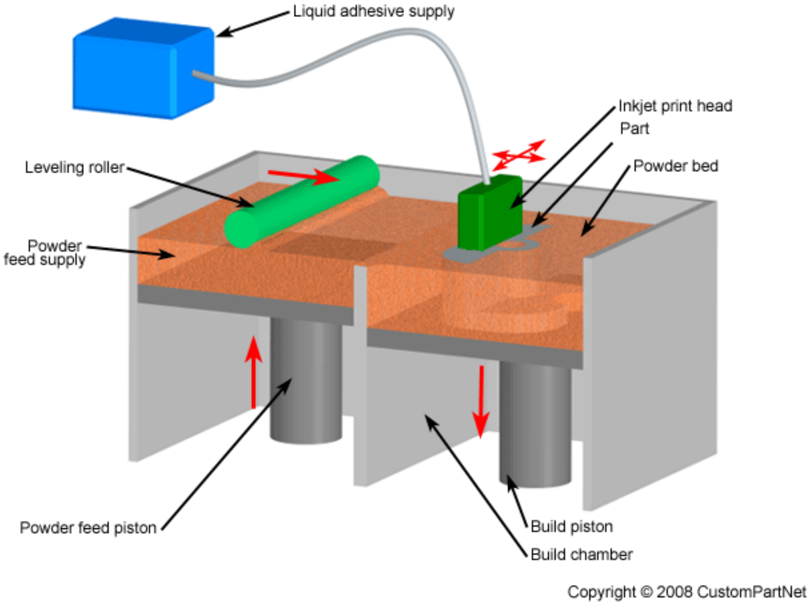

Figure 1.6 – Sketch of the powder-bond binding [6]

Fused Deposition Modelling (FDM)

Fused Deposition Modelling is a solid-based process where a thin filament of thermoplastic material feeds a machine. A print head melts it and extrudes it on the building platform. This extruder head moves in xy directions and traces the contour of the layer. The process continuously works since the filament feeds the machine (figure 1.7). The big advantages of this technique is that the object does not need further post-processing (curing resin e.g.) and does not need a laser.

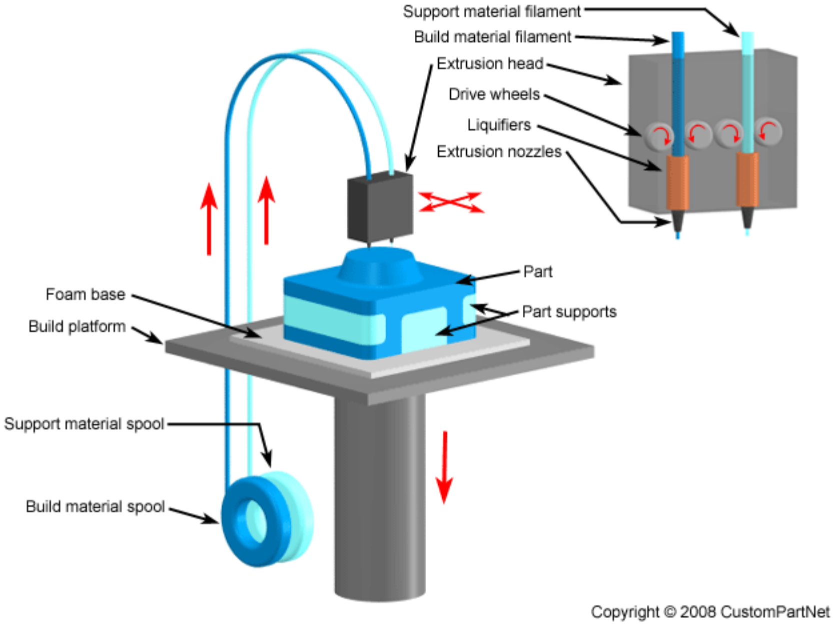

Figure 1.7 – Sketch of the fused deposition modelling [6]

Laminated Object Manufacturing (LOM)

Laminated Object Manufacturing is a solid-based process where sheets or foils are deposited on the building platform. A coating roller heats them and applies pressure to stick these foils together. Then a laser cut them into the form of the CAD-file as shown in figure 1.8. This cycle is repeated until the object is entirely built.

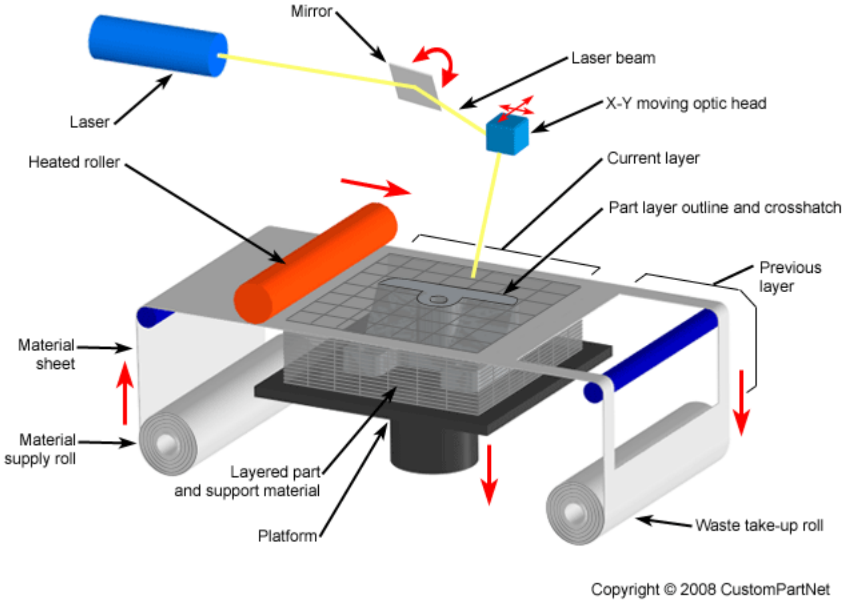

Figure 1.8 – Sketch of the laminated object manufacturing [6]

1.1.2 Steps of an additive manufacturing process

Processing an object with additive manufacturing technologies asks some steps before the preparation of the primary material. These steps are always the same for all technologies:

- Design of a 3D-model (CAD-file, for computer assisted design) with a 3D-modelling software.
- Conversion into a STL file format (standard format) and slicing the file into layers (with a chosen thickness).
- Importation in the device.
- Building the object layer by layer in z direction and mapping in xy plane.
- Removing the object out of the machine and post-processing (cleaning, curing, sintering, thermal treatment, ...).
- Application of the object.

1.1.3 Application areas

There are lots of application fields covering a large range of industries: aerospace (the goal is to reduce the weight), automotive industry (complex shape parts), defense, biomedical products (3D model bones before surgery, medical prosthesis, teeth aligners), health care, transportation, architecture, modelling (representation of reality), electronics (circuitry, conductors, insulators, ...), tooling, prototyping (idea of manufacturing cycle production, ...) and so on.

The criteria that make additive manufacturing useful for the specific fields are the possibilities to manufacture complex geometries and small size materials.

1.2 Photopolymers and photopolymerization

Photopolymers are polymers which present a light-induced polymerization. Electromagnetic radiation energy (visible light, UV) is converted into chemical energy (under reactive intermediates form like free radicals, cations, anions, ...) by a **photoinitiator molecule**. Then reaction begins and monomers and/or oligomers are bonded together to form a high molecular weight macromolecule [7]. Photoplymerisation has three steps:

1. **Initiation** of the process. This occurs with a photoinitiator molecule, which transforms light energy into chemical energy.
2. **Propagation** where radicals combine themselves with monomer/oligomer to form a long radical chain.
3. **Termination** to the end of the reaction by two possible paths: recombination or disproportionation.

There are two major polymerization systems: free radical polymerization and cationic polymerization. In this thesis, **free radical polymerization** is going to be used. Its advantages are fast curing, good storage stability, cheaper than cationic polymerization and it does not need post-curing [8]. The next subsections are focusing on free radicals.

1.2.1 Photoinitiation

Photoinitiators are divided into two groups:

- in the first type, an unimolecular bond cleavage is done due to the light and directly forms a free radical (it is called α-cleavage type photoinitiator).
- in the second type, a bimolecular reaction takes place: light excites the photoinitiator, its excited state interacts after with a second molecule and creates the radical. This type is called H-abstraction type photoinitiator.

Both cases are summarized by reaction {1} where PI is the photoinitiator and $R_i^{\bullet}$ is the formed free-radicals.

$$\mathrm{PI} \xrightarrow{h\nu} 2\,\mathrm{R_i}^{\bullet} \qquad \{1\}$$

1.2.2 Propagation

The radicals formed in initiation step react with the monomer units. Step by step, all the monomers are converted into a chain with a free radical at the end and form a high molecular weight radical. The propagation is characterized by the transformation of double bonds C=C into single bonds C−C as shown in reaction {2}.

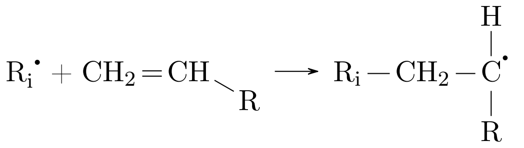

$$\mathrm{R_i}^{\bullet} + \mathrm{CH_2{=}CH{\diagdown}R} \longrightarrow \mathrm{R_i{-}CH_2{-}}\overset{\mathrm{H}}{\underset{\mathrm{R}}{\mathrm{C}^{\bullet}}} \qquad \{2\}$$

1.2.3 Termination

The end of the polymerization occurs when two radical chains meet each other. **Recombination** {3} happens when the two chains react together to form a longer chain.

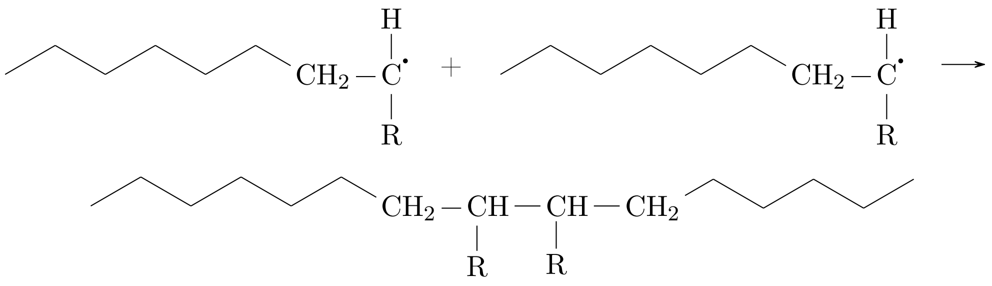

{3}

Disproportionation {4} appears when two different compounds are formed when the free radical chains react together. At the end, a high molecular weight crosslinked macromolecule is formed.

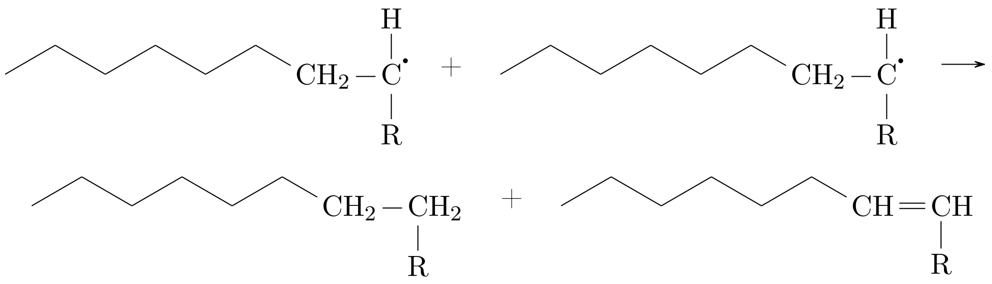

{4}

1.2.4 Applications

Photopolymers have lots of applications in different fields [9]. They are used in electronics (printed wiring boards, integrated circuits), printing (plates), optical materials (e.g. liquid crystal displays), for fabrication of devices, for adhesive (e.g. UV glue) and sealants, for coating and surface modifications (appearance and protection), inks (gravure, screen), medical applications (dental field, membranes), ...

1.3 Toughening of polymers and core-shell particles

Toughening polymers is important to increase their properties. Polymers usually present good properties in compression but low ones in tension, where they are brittle. Several mechanisms [10] can be used to improve mechanical properties: incorporation of rubbery particles, use of fibres, use of stress-activated plasticizing diluents [11] and of course incorporation of a new type of particles (the so-called **core-shell particles**).

1.3.1 Toughening mechanisms

Local mechanisms used to improve toughness of polymers are fully described in [10]:

- Multiple microcrack and void formation (creation of new surfaces by debonding microparticles).
- Bridging mechanism (dispersion of ductile particles into a brittle matrix).
- Multiple initiation of crazes or shear bands (dispersion of soft particles which have an effect of stress concentration).
- Nanovoid formation with yielding fibrillation (plastic yielding of the matrix between the nanovoids).

1.3.2 Core-shell particles

Core-shell particles are new impact modifiers used to enhance mechanical properties of polymers. They consist of a rigid shell and a soft core (figure 1.9). The shell ensures the compatibility between the matrix and the particles. When a crack reaches a core-shell particle, the polymer matrix absorbs impact energy while, around this particle, new smaller cracks are created. Energy is thus dispersed in a bigger volume and the initial crack will get stopped.

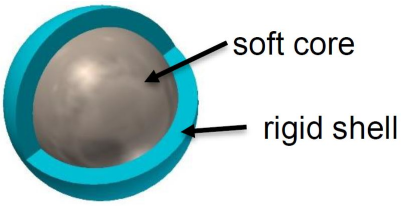

Figure 1.9 – Sketch of a core-shell particle [12]

1.4 Technical polymers

A photopolymer with good mechanical properties (elongation at break, impact strength) and good thermal properties (thermal stability) is needed. The following polymers are technical polymers which exhibit those properties.

1.4.1 ABS: Acrylonitrile Butadiene Styrene

One technical polymer which has the target properties is ABS. ABS is a modified two-phases thermoplastic composite polymer. It is made by grafting an elastomer butadiene-based material (figure 1.10c) with a matrix material consisting of an acrylonitrile-styrene copolymer (SAN, figures 1.10a and 1.10b).

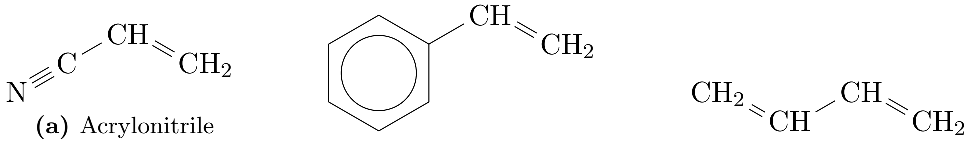

(a) Acrylonitrile

(b) Styrene

(c) 1,3-butadiene

Figure 1.10 – Chemical structures of ABS components

Three processes [13] are usually used to synthesize ABS: mechanical blending, bulk copolymerization and emulsion grafting. Properties of ABS depend on the process used to manufacturing. The rubber content also influences the properties (more rubber content means better tough properties) and temperature range in which ABS can be used. The morphologies of the different kinds of synthesized ABS are shown in figure 1.11. Soft "particles" of butadiene are embedded in a hard matrix.

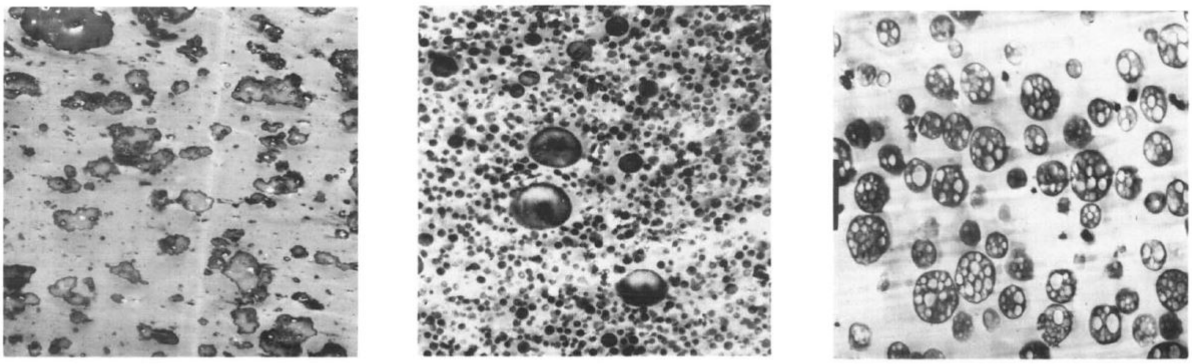

(a) Mechanically-blended ABS **(b)** Bulk-copolymerized ABS **(c)** Emulsion-grafted ABS

Figure 1.11 – Microscopies of ABS [13]

Due to its two phase nature, it has very good ductile properties, high toughness and high impact strength [14]. It has thermal stability and good chemical resistance against lots of compounds (except for ketone, aromatic and chlorinated hydrocarbon where it is soluble). Advantages of ABS are biocompatibility and cheapness. ABS becomes yellow when it is exposed to light, weathering conditions or oxidation. Nevertheless it losses toughness properties with time.

ABS can be processed with different technologies as for example injection moulding, extrusion, electroplating. In additive manufacturing, fused deposition modelling is one of the most common techniques [15]: the wire of ABS is guided into the head extruder, where it is molten. The liquid is then deposited layer by layer on the building platform.

ABS covers a large field of applications:

- Protective headgears like motorbike helmets.
- Sport: golf club heads.
- Household and consumer goods as washing machine, air conditioning, electric shavers, vacuum cleaners, ...
- Automotive industry: radiator grilles, instrument panels, body of *Citroën Méhari*, motorised quadricycle.
- Travelling: luggages, caravans.
- Toys, including Lego and Kre-O bricks.

1.4.2 PC: Polycarbonate

Polycarbonates are linear thermoplastic polyesters. Figure 1.12 represents the chemical structure: bisphenol A units are linked together by a carbonate.

Synthesis is not really difficult: it comes from the polycondensation of bisphenol A (BPA) and a carbonate or a phosgene (chemical compound with formula $COCl_2$. Two hydrogens of BPA react with chlorine atoms of the phosgene: this polycondensation reaction releases $2 \cdot n$ HCl molecules [16].

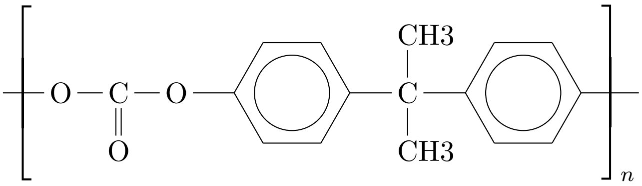

Figure 1.12 – Chemical structure of Polycarbonate

PC has very large range of good properties. It has a high impact strength as well as a good thermal resistance. Optical and electrical insulating properties are good. PC exhibits good toughness and rigidity until 140 °C. Unfortunately, manufacturing and production are expensive.

Processing is done by extrusion or by injection moulding between 240 °C and 300 °C.

As for ABS, applications are numerous [17], [18]:

- Electronics and electrical engineering: batteries, relays, covers for time switches, plugs, sockets, ...
- Automotive industry: wing mirrors, turn signals, lights, ...
- Telecommunication field: telephone switching mechanisms, data storages (CD, DVD), ...
- Security components: laboratory safety goggles, smartphone cases, helmets, visor of lunar astronauts, ...
- Construction materials: sheeting in a greenhouse.
- Domestic applications: food bowls, bottles, microwave doors, coffeemaker cold water reservoir, vacuum cleaner, hair driers, ...

1.4.3 PPSU: Polyphenylsulfone

Polyphenylsulfone is a high-performance polymer belonging to the family aromatic polyethersulfone. It contains aromatic rings, which are connected together by sulfone groups and by ether-bridge as shown in figure 1.13. PPSU is also known under its commercial names: Radel® from Solvay [19] and Ultrason® P from BASF Plastics [20].

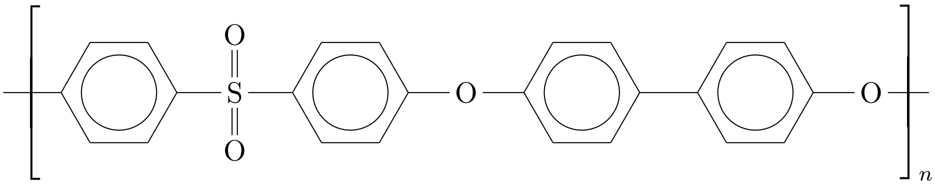

Figure 1.13 – Chemical structure of Polyphenylsulfone

PPSU is made by polycondensation of a bisphenol and a sulfone material (usually 4,4'-bis(chlorophenyl)sulfone).

PPSU is an amorphous polymer [21] having good mechanical properties (high tensile and impact strengths) and resists against chemicals, heat (stability at high temperatures) and high-energy radiations. It also has good electric and dielectric properties.

Processing of PPSU is usually done by injection moulding or by extrusion between 120 °C and 160 °C. Rapid prototyping can also be used for processing PPSU.

PPSU has a lot of applications in different fields [22]:

- Automotive industry: head lamps, headlights, interior reflectors, ...
- Household sector: non-stick coated pan, microwave dishes, ...
- Electronics: computer parts, insulation, electrical switch parts, capacitor films, ...
- Plumbing/sanitary: rolls, valves, fittings, ...
- Visor for fire helmets.
- Bio-engineering: instruments requiring hot air and steam sterilization.
- Impact strength modifiers for composite materials and binder materials.

Chapter 2

Method

The following steps are needed to obtain the information about the thermomechanical properties of the final parts:

- Preparation of the formulation, which consists of mixing the resin with the core-shell particles and the master batch. It is followed by a degassing to avoid air contamination.
- 3D-Printing of the polymer mixture into different samples.
- Post-curing, where printed polymers are cleaned in an oven and then stabilized in a UV-chamber.
- Mechanical, thermal and chemical tests [23].

2.1 Preparation of the polymer mixture

2.1.1 Classical way

The mixing of the polymer resin and the core-shell particles is done in a stirrer reactor (figure 2.1) during 24 h at a temperature around 95 °C. This temperature is needed to decrease the viscosity of the resin and thus to have a good particles distribution.

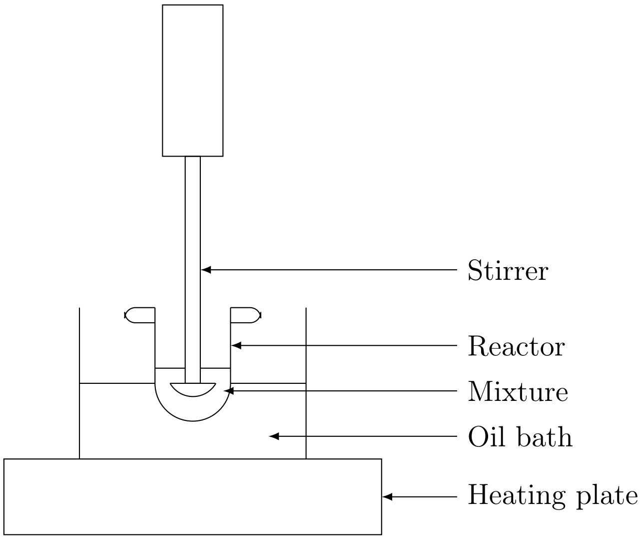

Figure 2.1 – Stirrer reactor

After this mixing, the *master batch* (containing the photoinitiator, the UV-absorber and the diluent) is added into the reactor and the whole is mixed for approximatively 1 h. The UV-absorber is used to enhance resolution of the printed objects.

A degassing is then done. It is very important because the mixture contains lots of air bubbles. These bubbles are not good for dimensionality of the samples and decrease properties. This degassing is done in a vacuum chamber at high temperature (around 95 °C). It is completed until the mixture becomes more transparent than before the degassing.

2.1.2 New approach: use of SpeedMixer

SpeedMixer is a dual asymmetric centrifugal mixing at high rotation speed: all compounds are mixed together simultaneously into a recipient at the speed of 3500 rpm for a few minutes. As the mixture must be heated, the recipient is placed into the oven at around 90 °C before mixing.

The biggest advantage of this technique is that the mixing is really faster than with the classical way but it is only possible if viscosity is low enough at high temperature. Nevertheless it is not possible, for the moment, to do the degassing in the same time. The transfer of the mixture into glass recipient is done and it is degassed into the vacuum chamber.

To visualize if the distribution of the particles is homogeneous, a mixture, containing 10 wt% particles has been prepared and cast into a rectangular form. This sample has been broken and the fracture was observed with the SEM. Figure 2.2 shows that the particles distribution is good after SpeedMixer. This means that this technique can be used for preparation of the different formulations.

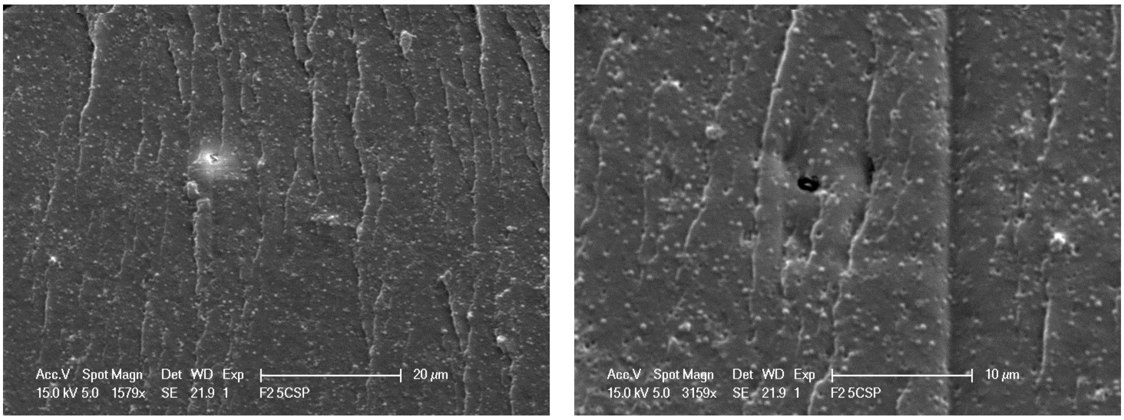

(a) 1579x **(b)** 3159x

Figure 2.2 – SEM pictures of a sample prepared with SpeedMixer

2.2 3D-Printing

The polymer can now be printed: BP7-device (Blue Printer 7) is used with a laser which has a wavelength of 375 nm and a specific power of 70 mW. CAD-files are imported in *.stl*-file. There are lots of parameters which can be changed to perform the printing:

- temperatures of the material vat, of the building platform, of the coating blade.
- motor parameters like the height of the coating blade or the down- and up-speed of the building platform.

- process parameters like the layer thickness or the force applied during the first layer.
- laser parameters like the scanning speed or the directions in which the polymerization is done (hatching).

Figure 2.3 represents the 3D-printer. The running is the following: firstly, the material vat is filled with our formulation. Material is directly deposited on the vat with a plastic spatula. Secondly, the material vat moves from left to right and then returns at its initial position. At this point, the height of the formulation on the vat is set. Thirdly, the building platform goes down and reaches the vat. The first layer is controlled by the force given as input parameter while the next layers are achieved by the layer thickness given in the CAD-file. Finally, the laser is turned on and polymerizes the formulation into a solid material. The building platform can now go up with the polymerized layer. The lab has two building platforms: a bigger one (10 × 20 cm) and a smaller one (8 × 14 cm). The smaller one is used.

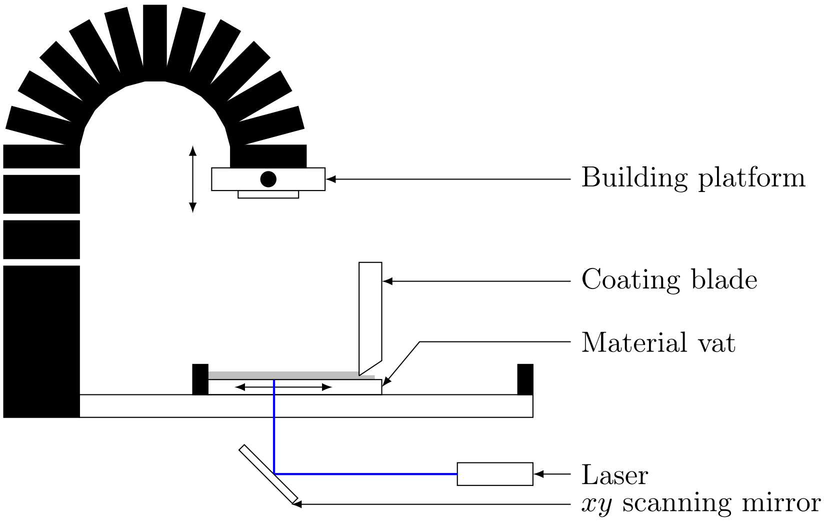

Figure 2.3 – Schematic drawing of the 3D-Printer

2.3 Post-curing

Post-curing contains two steps: the first one is a rapid cleaning in an oven at the temperature of 90 °C. It is done because there remains non polymerized mixture on the samples. At this temperature, samples are relatively easy to clean.

The second step is the "final" polymerization in the UV-chamber. Polymerization of the remaining non-cured formulation is achieved. Samples are placed into a chamber under nitrogen atmosphere to avoid oxygen contamination. Polymerization is done with 2000 flashes between 300 nm and 700 nm (with a rate of 10 flashes per second).

2.4 Mechanical, thermal and chemical tests

2.4.1 Charpy Impact Test

Charpy Impact Test allows the determination of the impact strength of a material. It works as following: a pendulum-hammer is thrown from a defined height in the direction of the sample, breaks the sample and goes up on the other side. The difference of heights before and after the sample is measured to calculate the impact strength. This strength is related to the absorbed energy into the sample when the collision happens. Figure 2.4a represents this test, the sample is drawn in red.

The samples have a length of 80 mm, a width of 10 mm and a thickness of 4 mm as shown in figure 2.4b. Single layers are represented by the dashed lines. Standard ISO 179-1 is followed.

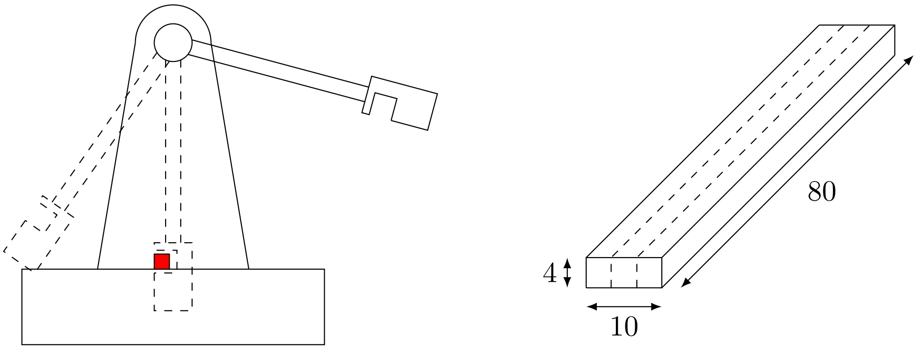

(a) Schematic draw of a Charpy impact test

(b) Sample sizes [mm] for Charpy impact test

Figure 2.4 – Charpy impact test

The used device directly gave the work needed to break the sample. The impact strength (a_c in $\mathrm{kJ\,m^{-2}}$) can be calculated by equation (2.1).

$$a_c = \frac{W_r - W_{\text{ref}}}{w \cdot t} \cdot 10^3 \tag{2.1}$$

where,

- W_r is the work read on the device in [J].
- W_{ref} is the work without any sample (as reference) in [J].
- w is the width of the sample in [mm].
- t is the thickness of the sample in [mm].

2.4.2 Tensile Test

Tensile test is a test used for the determination of mechanical properties such as Young's modulus, yield strength, maximal strength, elongation at break, ... Sample with form like drawn in figure 2.6 is clamped on both sides. A force (or a displacement) is applied to the sample, which will be deformed. Stress-strain curves are describing the system: stress σ is defined as the force divided by the area (equation (2.2)) and strain ε is defined as the elongation divided by the length of the sample (equation (2.3)). The subscript 0 means that the initial area and length are used.

$$\sigma = \frac{F}{A_0} \tag{2.2}$$

$$\varepsilon = \frac{\Delta l}{l_0} = \frac{l - l_0}{l_0} \tag{2.3}$$

Figure 2.5 shows the typical curves of three different kinds of polymers.

- The blue curve (A) represents a duroplast or a brittle polymer: elongation at break is low. In case of duroplast, yield strength is high.
- The green curve (B) represents a thermoplastic polymer or a tough-modified polymer: strength is lower than case A but elongation is much more higher.
- The red curve (C) represents an elastomer: a yield strength cannot be clearly defined but elongation at break is very high. Tensile strength is very low.

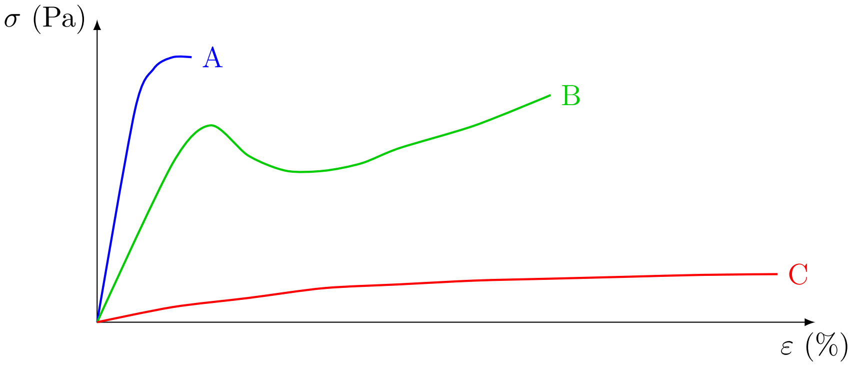

Figure 2.5 – Stress-strain curves for different kinds of polymers [23]

Table 2.1 gives the useful properties of a tensile test.

Table 2.1 – Useful information of a tensile test

	Symbol	Unit	Description
Yield strength	R_e	Pa	Limit between elastic and plastic domains
Maximal strength	R_m	Pa	Maximal point of the curve.
Young's modulus	E	Pa	Slope of the elastic domain.
Elongation at break	ε_b	%	Elongation just before break of material.

Elongation at break and maximal strength are the two interested parameters. The samples follow the dimensions from the Standard ISO 527-1 (geometry 5B), which are given in figure 2.6. Thickness of the samples is around 1 mm.

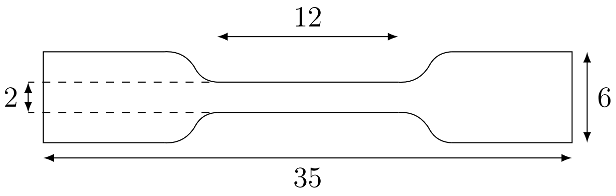

Figure 2.6 – Sample sizes [mm] for tensile test

2.4.3 DMA - Dynamic Mechanic Analysis

DMA is an analysis used for the determination of thermal properties (e.g. glass transition temperature, melting point, thermal stability) and mechanical properties (e.g. storage modulus, loss modulus) following a thermal cycle. In this method, a sinusoidal deformation is applied to the samples and the response of the system is analysed. The deformation is done by 3-points bending with the following parameters: 10 µm amplitude and 0.05 N pre-load force.

The thermal cycle consists of three legs: first an equilibrium at −50 °C, than an isothermal at −50 °C during 5 min following by a temperature ramp until 150 °C (temperature increase is $3\,°\mathrm{C\,min^{-1}}$). The samples dimensions are given in figure 2.7.

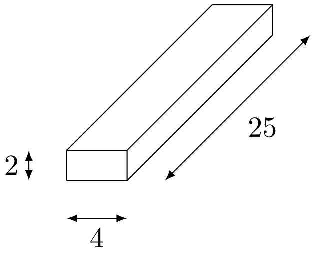

Figure 2.7 – Sample size [mm] for DMA

Young's modulus (E^*) and shear modulus (G^*) are imaginary numbers:

$$E^* = E' + iE''$$
$$G^* = G' + iG''$$

The real part is called **storage modulus** while the imaginary part is called **loss modulus**. The ratio between the two moduli gives the so-called tangent delta (equation (2.4)) with which it is easily to determine the glass transition temperature.

$$\tan\delta = \frac{E''}{E'} = \frac{G''}{G'} \tag{2.4}$$

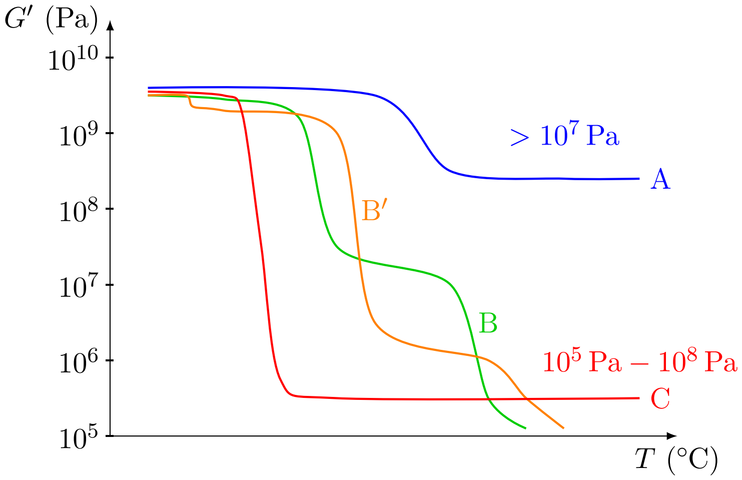

Figure 2.8 – Modulus-Temperature curves for different kinds of polymers [23], [24]

Figure 2.8 gives the ideal curves of different kinds of polymers. For all polymers, the first part of the curve is a **glass zone**. Then follows the **glass transition zone** where the polymer goes from a rigid state to a soft state. It is then possible to have a **rubber level** (elastic entropic behaviour). The last part is the **fluid flowing zone**.

- The blue curve (A) represents a duroplast: the storage modulus has a small step but it remains quite high ($> 10^7$ Pa). Glass transition temperature is the inflexion point of the step. It is used below its glass transition temperature.

- The green curve (B) represents an amorphous thermoplastic polymer: the four legs can be seen. This kind of polymer is used below the glass transition zone.
- The orange curve (B′) represents a semi-crystalline thermoplastic polymer: the glass transition zone is very tiny and appears at low temperature. Then a energy-entropy behaviour appears (plateau at high modulus) before a melting zone (first big drop of the curve). The last part is the fluid flowing zone.
- The red curve (C) represents an elastomer: the transition from a rigid state to a soft state is steeper than for duroplasts. Unlike duroplasts, it is used above its glass transition temperature.

2.4.4 Viscosity Measurements

Viscosity of polymer mixture must be tested before printed to be able to choose a proper temperature range. For a good printing, the viscosity must be lower than 20 Pa s. Measurements have been done with a rheometer from 50 to 110 °C with a ramp of 3 °C min^{-1}. A plate plate set-up is used: the gap is 200 µm and the shear stress is 50 s^{-1}. Figure 2.9 represents the viscosity measurement: the two plates are placed into a heating room (sample is drawn in grey).

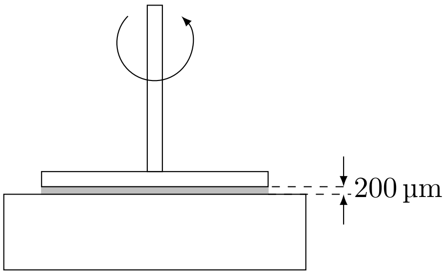

Figure 2.9 – Set-up of the viscosity measurements

2.4.5 Double Bond Conversion Test

Double bond conversion test gives the number of double bonds C=C which have been converted into single bonds C−C. As shown in figure 2.10, the absorbance is measured with an infra-red light for an uncured material and for a printed (cured) material. At the wavenumber of the C=C bond (around 6150 cm^{-1}), the ratio between the areas below the two curves is made and the double bond conversion (DBC) is calculated by equation (2.5).

$$DBC = 1 - \frac{A_{\text{uncured}}}{A_{\text{cured}}} \tag{2.5}$$

Cured samples have a circular form with a diameter of 20 mm and a thickness of 500 µm. A mould with these dimensions is used for the uncured material which is still liquid.

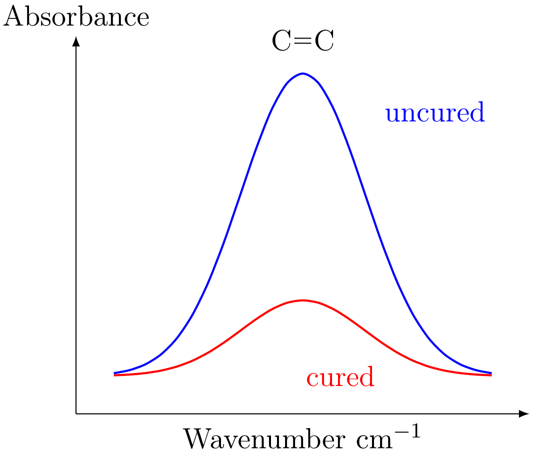

Figure 2.10 – Double bond conversion

Chapter 3

Results

Results are divided into four parts which have a different aim. The first part has been done to see the influence of core-shell particles on mechanical properties (typically elongation at break and impact strength). In the second part, another material will be used with the goal to increase again elongation at break and impact strength. In part III, a research of new mixtures has been carried out by casting the samples: two different formulations have been printed and analysed by thermal and mechanical tests. The last part will study the influence of a cross-linker on mechanical and thermal properties.
Seven tensile and nine Charpy samples have been printed for every formulation. The average value and the standard deviation have been calculated. A summary of all formulations is available in appendix A. All materials used during this thesis are described in detail on appendix B.

3.1 Part I: influence of core-shell particles on a commercial resin

3.1.1 Materials

In this part, the following materials are used:

- Resin: commercial difunctional acrylate with a glass transition temperature around 110 °C.
- Core-Shell particles: PMMA shell, PBA core, diameter around 200 nm (from 0.0 wt% to 20 wt%).
- Master batch containing UV-absorber (0.1 wt%), photoinitiator (0.6 wt%) and reactive diluent (0.6 wt%).

Printings are done with two different layer thickness (100 µm and 50 µm) and results in both cases will be compared. Samples are named XRxx.

3.1.2 Results

Different samples have been printed with increasing core-shell particle amount from 0 to 16.5 wt% and those have been tested with the different tests. The first test to make is the viscosity measurements: results are given in figure 3.1. Viscosity becomes higher when the amount of core-shell particles increases. Interested temperature range is between 75 and 95 °C where the viscosity is lower than 20 Pa s. For this system, a temperature of 90 °C is fine for printing. At higher temperature, acrylate systems have a thermal curing which is to avoid.

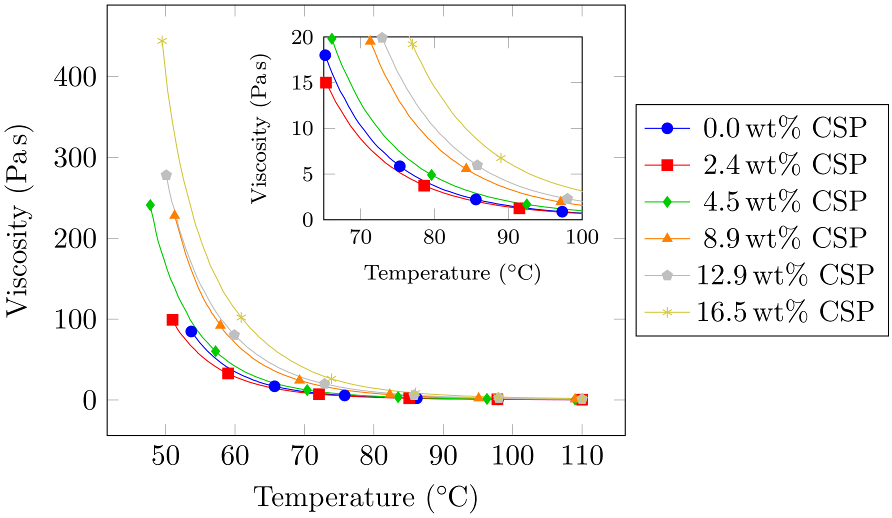

Figure 3.1 – Evolution of the viscosity as function of the temperature with different amounts of core-shell particles (commercial resin)

Double bond conversions are given in table 3.1. The conversion is quite high for all samples, which means that the polymerization was efficient. Lots of the monomer/oligomer units have been converted into longer chains.

Table 3.1 – Double bond conversion (in %) as function of the core-shell particles amount for 100 µm thick samples

CSP amount (wt%)	0.0	2.4	4.5	8.9	12.9	16.5
DBC (%)	85	93	93	91	96	90

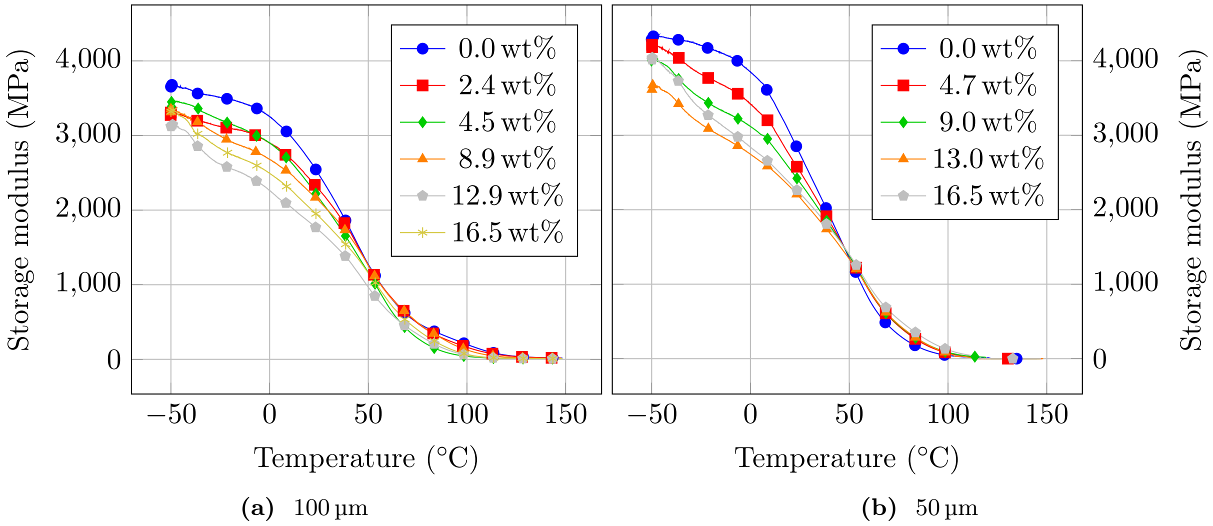

(a) 100 µm **(b)** 50 µm

Figure 3.2 – Evolution of the storage modulus as function of the temperature with different amounts of core-shell particles (commercial resin)

DMA curves (figure 3.2) show that the storage modulus decreases when the amount of particles increases. Glass transition temperature is not really affected by the core shell particles and varies between 100 °C and 115 °C. Lower layer thickness gives higher storage moduli.

Mechanical tests are given in figure 3.3 where Charpy impact test measurements have been done with different hammers:

- 100 µm: from 0.0 wt% to 8.9 wt%, the hammer 0.5 J is used while the hammer 1 J is used for the two other samples.
- 50 µm: the 0.0 wt% sample has been tested with hammer 0.5 J; from 4.7 wt% to 13.0 wt%, hammer 1 J; hammer 2 J for 16.5 wt% sample.

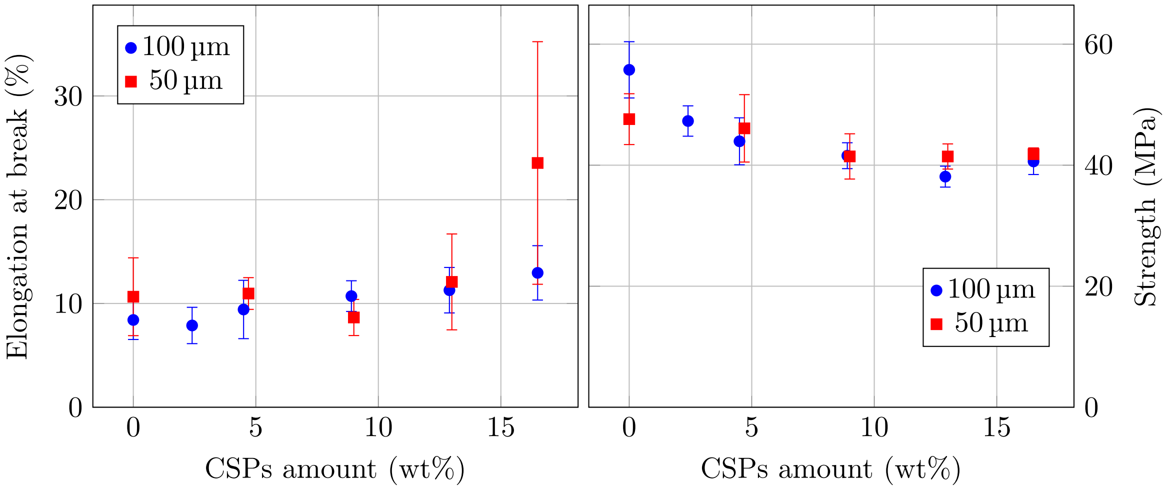

(a) Elongation at break

(b) Maximal strength

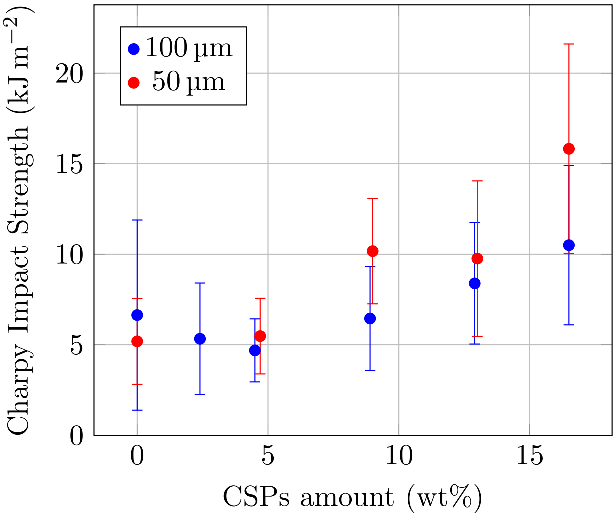

(c) Charpy impact strength

Figure 3.3 – Mechanical tests results as function of the core-shell particles amount (commercial resin)

Strength decreases a little with the particles content while elongation at break increases. Influence of the core-shell particles is noticeable but the improvements are not really big. Decreasing layer thickness increases elongation at break and Charpy impact strength but quite a lot of particles are needed (more than 15 wt%) to have a significant improvement. Figure 3.4 gives examples of printed tensile and DMA samples.

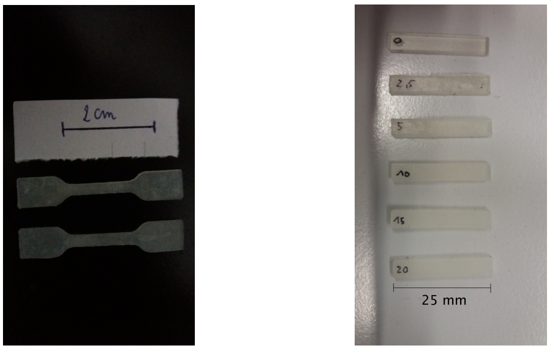

(a) Tensile samples for 12.9 wt% CSPs

(b) DMA Samples (commercial resin)

Figure 3.4 – Tensile and DMA samples

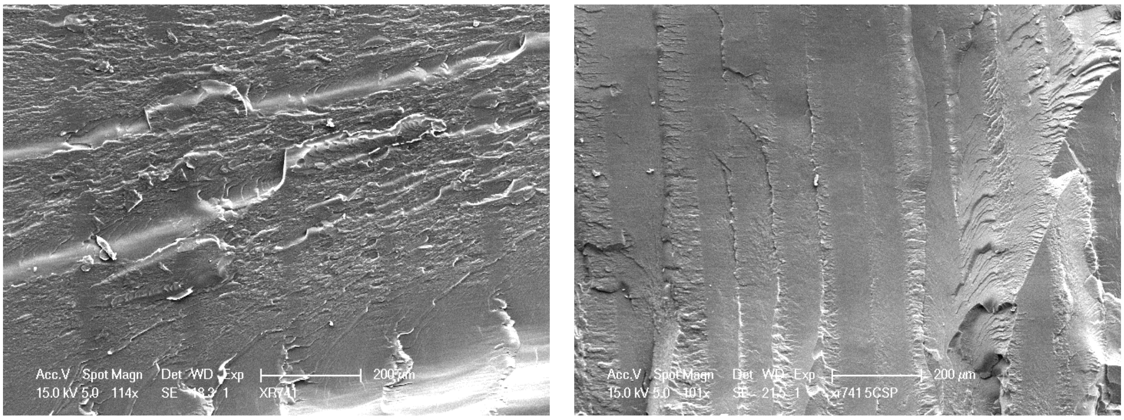

(a) XR00 (0.0 wt% - 100 µm)

(b) XR05 (4.5 wt% - 100 µm)

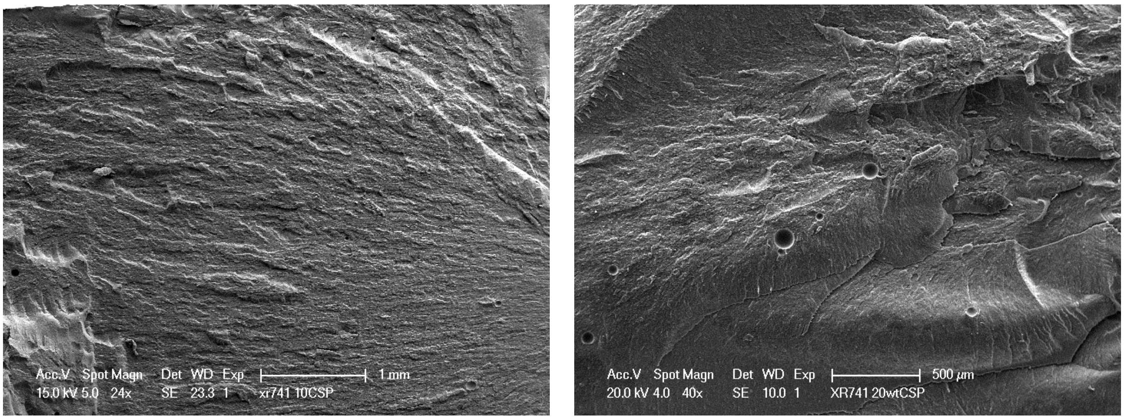

(c) XR20 (8.9 wt% - 100 µm)

(d) XR20 (16.5 wt% - 100 µm)

Figure 3.5 – SEM pictures of fractures from Charpy impact tests with 100 µm layer thickness (commercial resin)

Figure 3.5 shows the fracture pictures of the Charpy samples. Samples have been analysed with the scanning electron microscope (SEM). The fractures are rougher for high particles content, which means that they are more ductile. Unfortunately, the information of single layers (vertical lines of pictures 3.5a and 3.5b for instance) are seen, which is not a good sign. Indeed, if the samples are pulled up in the direction of these single layers, they might not stick well together and thus mechanical properties are decreased.

When decreasing layer thickness (figure 3.6), the single layers cannot be seen and thus the properties are better. Moreover, it is seen, on figure 3.6a, that the fracture is very smooth in comparison to figure 3.6c. Mechanical properties of the polymer without particles are thus low.

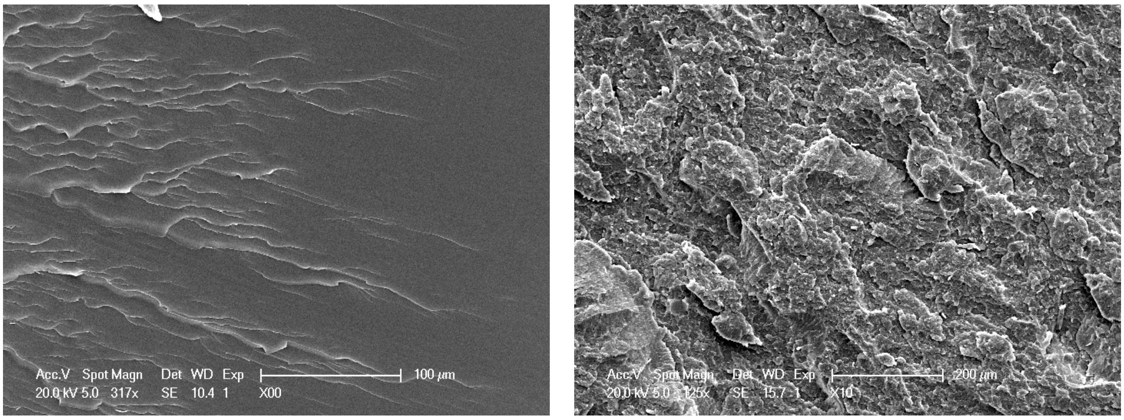

(a) XR00 (0.0 wt% - 50 μm) **(b)** XR10 (9.0 wt% - 50 μm)

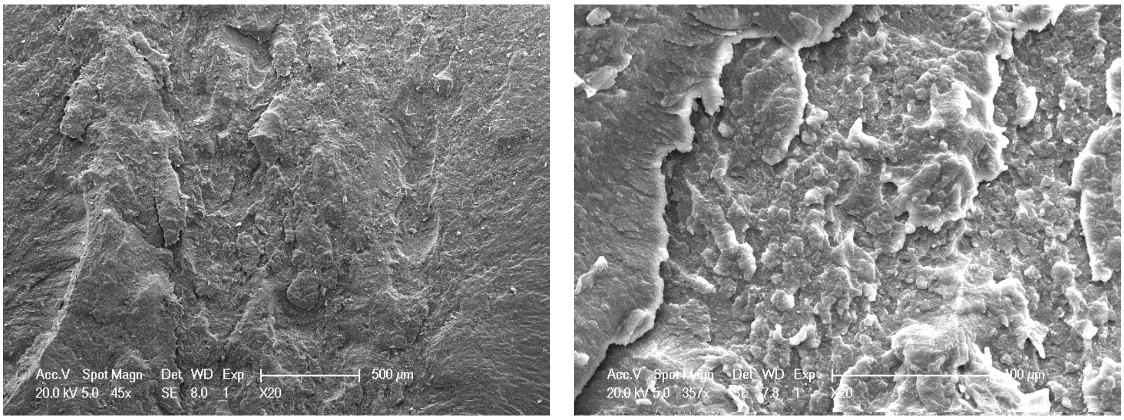

(c) XR20 (16.5 wt% - 50 μm) **(d)** XR20 (16.5 wt% - 50 μm)

Figure 3.6 – SEM pictures of fractures from Charpy impact tests with 50 μm layer thickness (commercial resin)

3.1.3 Summary

The conclusion of this first part is that core-shell particles help to improve the mechanical properties. The problem of the used resin is that it is highly cross-linked. This high content of cross-linking makes the material brittle. It is why, in part II, another type of formulation will be prepared. This formulation should have a lower cross-lining content.

A second information given by part I is that decreasing layer thickness improves the properties. The major drawback of decreasing this thickness is that printing takes longer time.

3.2 Part II: modification of the polymer resin and influence of the scanning speed

3.2.1 Materials and preparation

In this part, another formulation is used. Two different resins are mixed together:

- a high molecular weight aliphatic difunctional acrylate which has good adhesion properties, high elongation but poor tensile strength. The molecular weight is around 20 000 g mol^{-1}.
- a high T_g methacrylate with a molecular weight around 1000 g mol^{-1}, used as cross-linker.
- particles and master batch are the same than in part I.

The preparation of this mixture is a little bit more complex because it needs the separation of two components from the high molecular weight material. This is done in three steps:

1. Dissolution of the resin into acetone (with magnetic mixing).
2. Drop by drop, put the mixture into a petrol ether solution and take the polymer.
3. Heat up the polymer until all solvent is evaporated.

After this separation, the resin is mixed with the high T_g material. Master batch and core-shell particles are added and then the whole mixture is heated in the oven to decrease its viscosity. SpeedMixer is used for mixing and formulation with ratio 40:60 (Mod4600xx) has been printed. To reduce the cross-linking, addition of monofunctional diluent in the formulation (Mod460500) has been tested.

3.2.2 Results

As for part I, the first test is the viscosity measurements. This is done to have the idea of the printing temperature. Layer thickness is set at 50 µm.

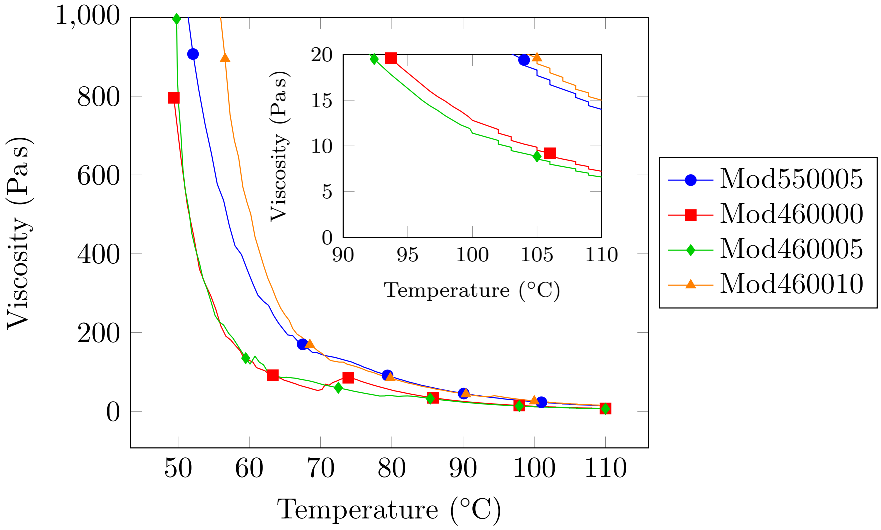

Figure 3.7 – Evolution of the viscosity as function of the temperature with different amounts of core-shell particles (modified resin)

As shown in figure 3.7, viscosity is higher than for the commercial polymer. Higher temperature is thus needed to print this formulation and one between 100 °C and 110 °C is chosen.

As seen in figure 3.8, samples with 5 wt% monofunctional diluent (Mod460500) and reference sample (Mod460000) have the same storage moduli for all temperature range. This probably means that the diluent is getting evaporated while printing. Addition of core-shell particles decreases the storage modulus. Glass transition temperature is around 120 °C (±5 °C).

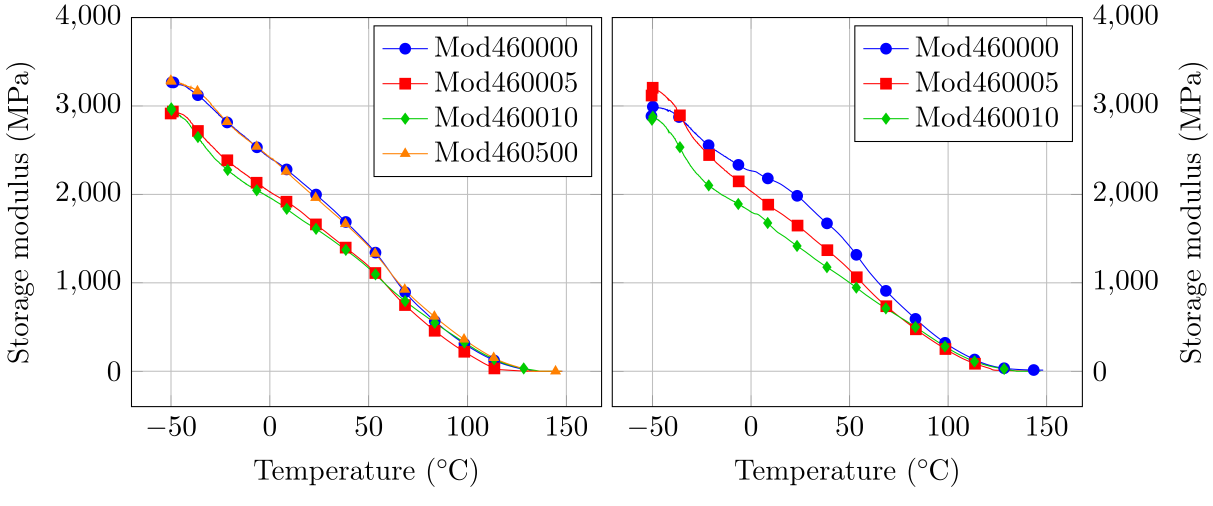

(a) Medium speed **(b)** Low speed

Figure 3.8 – Evolution of the storage modulus as function of the temperature (modified resin)

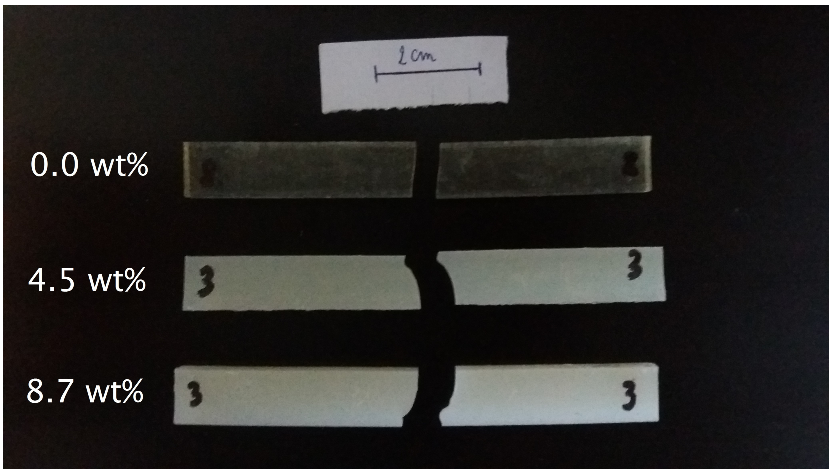

Figure 3.9 – Charpy samples after testing (Mod460000, Mod460005 and Mod460010)

Figure 3.9 represents three samples from the modified resin after testing by Charpy impact test. Addition of particles makes the polymer white. Mechanical tests are given in figure 3.10. Addition of monofunctional diluent does not improve the mechanical properties. Decreasing the scanning speed of the laser has been investigated to have its influence on mechanical properties but here again, they are not really affected. Charpy impact tests are worst with a low scanning speed. Hammer 1 J has been used for all samples.

SEM pictures of impacts tests have been done and are given in figure 3.11. It is still possible to see single layers but only for reference material (without particles). The other pictures show

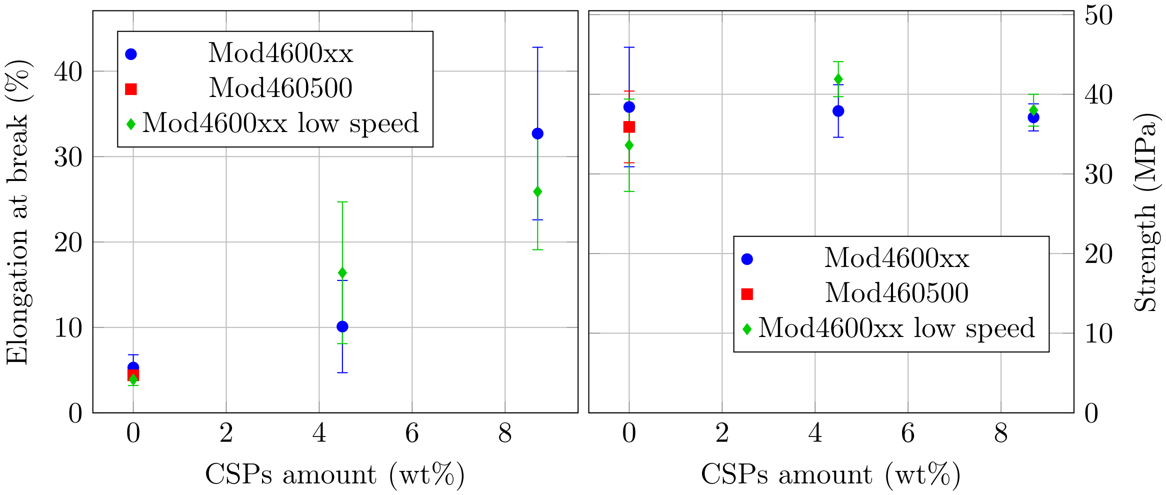

(a) Elongation at break

(b) Maximal strength

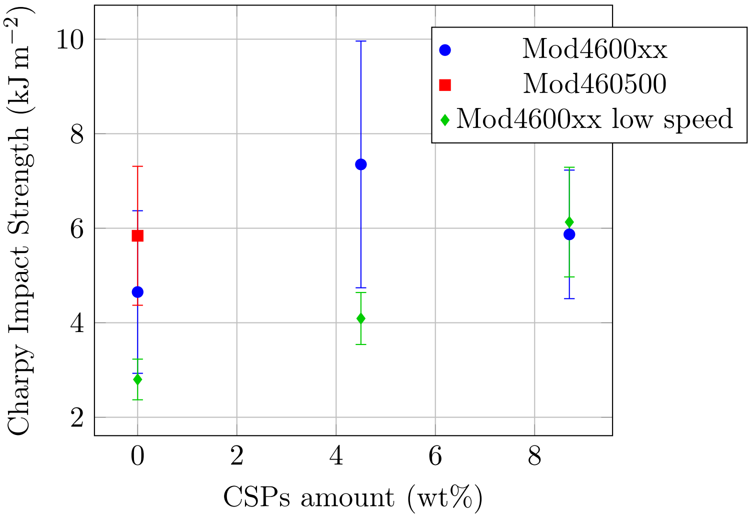

(c) Charpy impact strength

Figure 3.10 – Mechanical tests results as function of the core-shell particles amount (modified resin)

a good particles distribution since agglomerations cannot be seen.

3.2.3 Summary

To finish this part, the new formulation (which consists of mixing two different compounds with 40:60 ratio) gives better results than the commercial resin with a lower core-shell particles content. Elongation at break can reach 30 % with only 10 wt% particles while the commercial resin needed at least 16 wt% to reach this value. The Charpy impact strength was really affected by the particles but the values remain poor (lower than 10 kJ m^{-2}. Thermal properties of this material are lower than those of the commercial resin.

Core-shell particles improve properties in a good way but the big drawback of this formulation is that the starting points (the properties without particles) are low. In the next section,

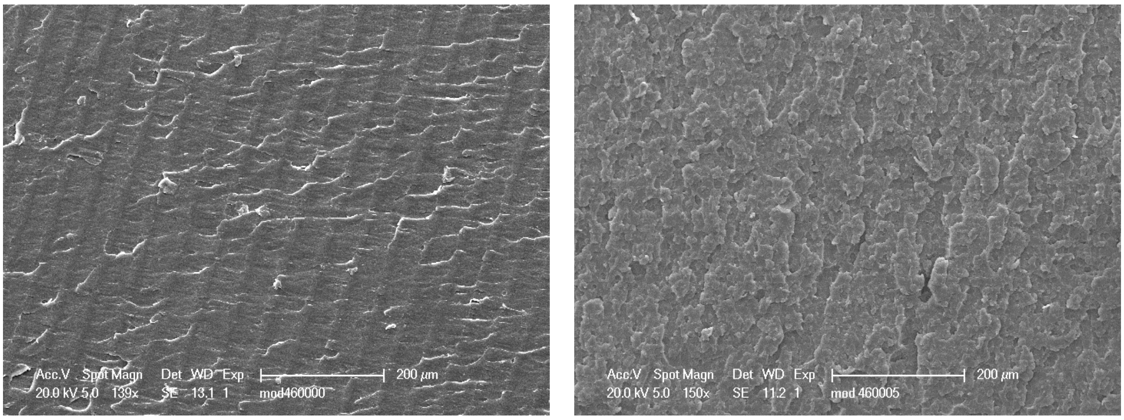

(a) Mod460000 (medium speed) **(b)** Mod460005 (medium speed)

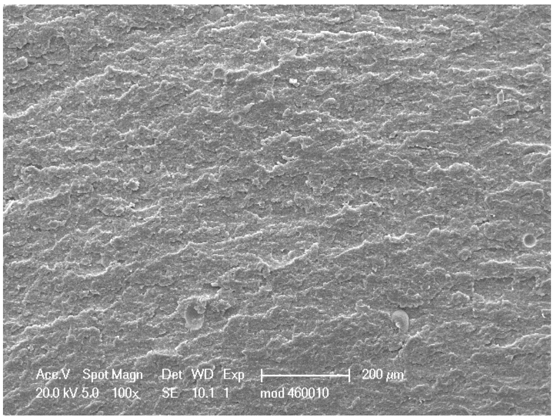

(c) Mod460010 (medium speed)

Figure 3.11 – SEM pictures of fractures from Charpy impact tests (modified resin)

investigation of other materials which could have better starting points is done.

3.3 Part III: search for a new material

3.3.1 Materials

As materials of part II did not have a good starting point (elongation at break without particles was too low), a research of new formulation has been done. Materials have been chosen in a list with the following criteria: glass-transition temperature higher than 40 °C and a molecular weight higher than $400\,\mathrm{g\,mol^{-1}}$. Those resins have been mixed with the high T_g cross-linker. Materials have been cast and have been manually broken to have a feeling of their flexibility and their brittleness. In table 3.2, all tested formulations are given: column ratio represents the mass ratio between the resin and the cross-linker (Resin:Cross-Linker).

Table 3.2 – Investigation of different resins

Material	Ratio	Comments
S146	40:60	highly brittle
S155	50:50	low flexibility
S164	60:40	little flexible
S173	70:30	little flexible
S246	40:60	flexible but brittle fracture
S255	50:50	more flexible but brittle
S264	60:40	little flexible
S346	40:60	brittle
S355	50:50	little flexible but brittle
S364	60:40	little flexible but brittle
S446	40:60	flexible
S455	50:50	flexible
S464	60:40	nicely flexible
S564	60:40	little flexible
S582	80:20	little flexible
S682	80:20	little flexible
S610	100:0	little flexible
S782	80:20	little more flexible than S682
S710	100:0	little more flexible than S610
S864	60:40	brittle
S882	80:20	brittle
S810	100:0	brittle
B55	50:50	flexible
B10	100:0	highly flexible

Only two formulations were nicely flexible and have been printed. The other resins were too brittle and have been rejected.

- Aliphatic urethane diacrylate (data S464x, S455x, S446x).
- Aliphatic urethane acrylate (data B55x) with good creep resistance.

Both materials will be mixed with the high T_g cross-linker used in part II. Same master batch and particles are used than in parts I and II. Only DMA and tensile tests have been done for these two formulations

3.3.2 Results

The tensile results are presented on figure 3.12. B55x formulations look quite promising: elongation without particles is high and this elongation is getting improved from 50 % to 75 % while the maximal strength remains more or less constant (this formulation shows a large plastic deformation during the tensile test). The diacrylate formulations are less affected by the particles: improvement is present but very tiny. Figure 3.13 gives the storage modulus curves of all printed samples. As for the other formulations, addition of core-shell particles decreases the moduli. Unfortunately, the shape of these curves are not really nice: the curves are too steep, which means that properties strongly depend on the temperature.

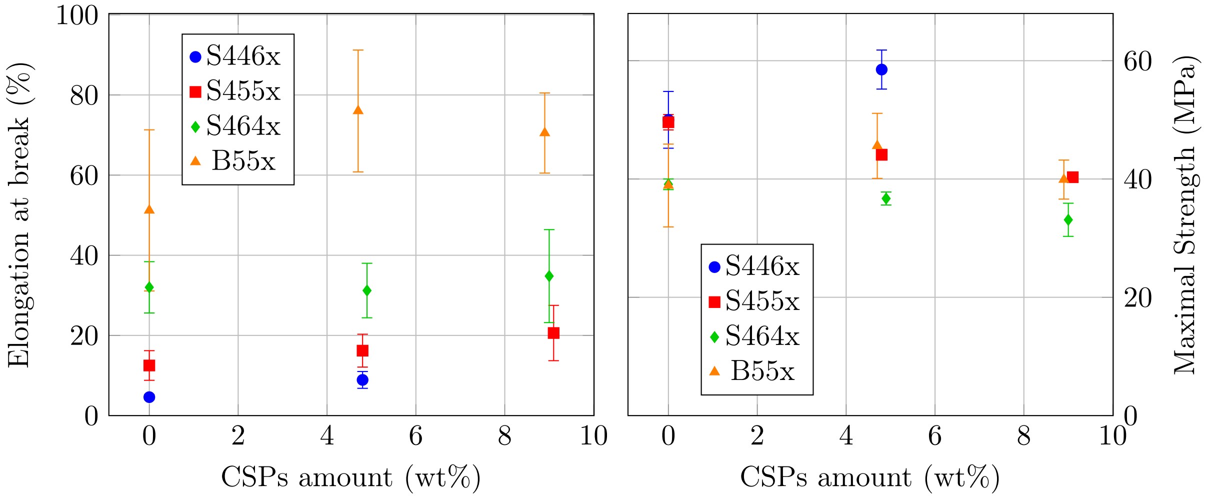

(a) Elongation at break

(b) Maximal strength

Figure 3.12 – Tensile tests results as function of the core-shell particles amount

3.3.3 Summary

The two new tested formulations exhibit a better starting point in elongation at break. Two of them were mixed with the cross-linker and printed. Elongations at break are 50 % for B550 (acrylate, ratio 50:50) and 37 % for S4640 (diacrylate, ratio 60:40). Acrylate material presents an improvement of properties when core-shell particles are added. However, the diacrylate material only admits a low improvement (from 32 % to 35 % for 60:40 ratio and from 12.5 % to 20.5 % for 50:50 ratio). Thermal properties of this two different resins are not that good since the slope of the storage modulus is high. Thermal stability is thus the drawback of these resins.

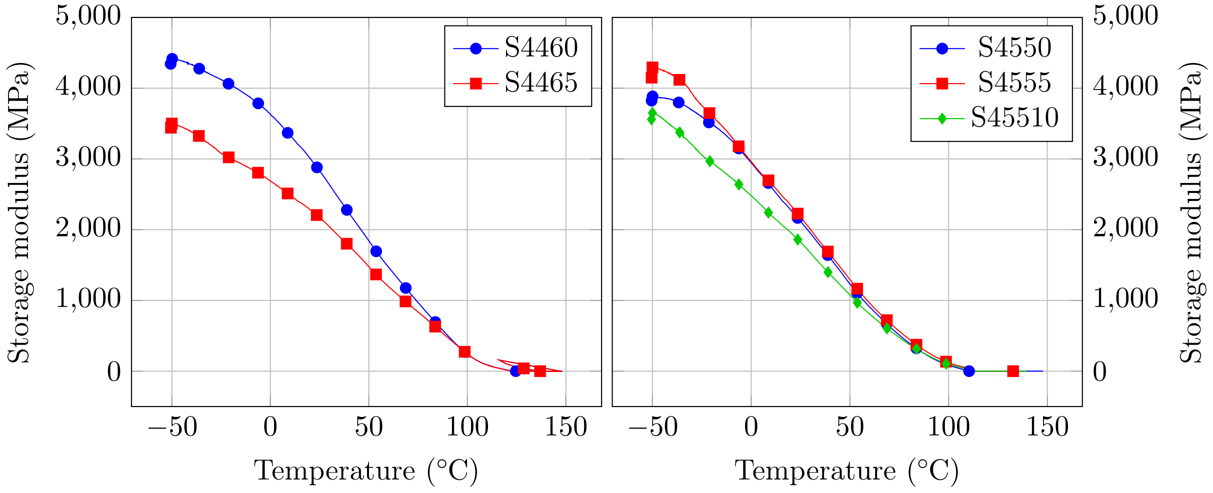

(a) S446x **(b)** S455x

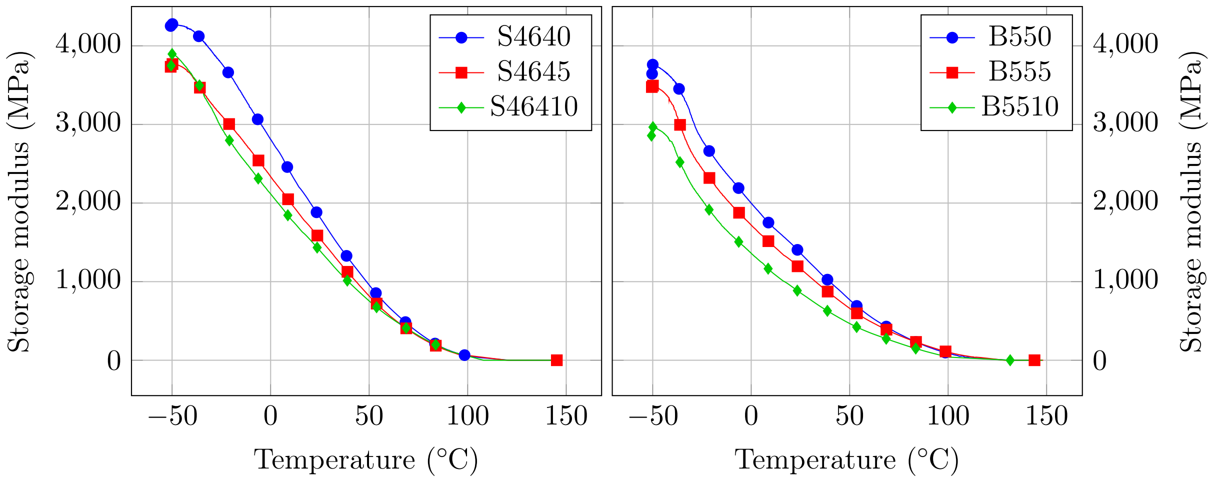

(c) S464x **(d)** B55x

Figure 3.13 – Evolution of the storage modulus as function of the temperature with different amounts of core-shell particles

3.4 Part IV: influence of the high T_g cross-linker

3.4.1 Materials

In this part, the influence of the high T_g cross-linker on mechanical and thermal properties will be discuss. Two formulations are tested:

- High molecular weight aliphatic diacrylate - data Mod370005 (30:70), Mod460005 (40:60) and Mod550005 (50:50).
- Aliphatic urethane diacrylate - data S4280 (20:80), S4460 (40:60), S4280 (50:50) and S4640 (60:40).

3.4.2 Results

As shown in figure 3.14a, elongation at break decreases for all formulations when the content of cross-linker increases. Due to its highly cross-linking, polymer becomes more brittle and elongation is very low. Figure 3.14b shows that maximal strength admits a maximum. Before this maximum (at lower cross-linker content), strength is low because the strength of the other resin is low. After the maximum, the polymer is brittle and breaks after a few seconds, strength is thus very low.

A short remark concerning formulation Mod550005: Charpy impact tests have been done and this formulation exhibits high impact strength (one sample did not break with the bigger hammer). Mod550005 reaches a high elongation at break ($59.9 \pm 9.9\,\%$), a decent maximal strength of $35.3 \pm 2.7\,\mathrm{MPa}$ and a high Charpy impact strength ($57.2 \pm 22.7\,\mathrm{kJ\,m^{-2}}$). One of the Charpy sample did not break with the 4 J hammer, which is the bigger one. This formulation is very good on the side of mechanical properties but thermal ones are poor: its storage modulus is low.

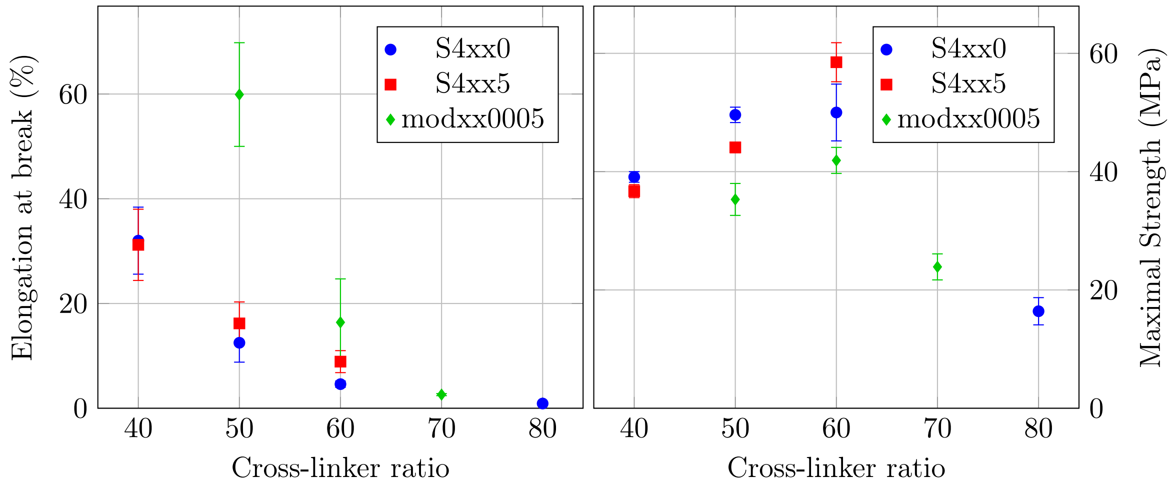

(a) Elongation at break **(b)** Maximal strength

Figure 3.14 – Tensile tests results as function of the ratio between resin and cross-linker

As given in figure 3.15a, the formulation with the most cross-linker (S4280) has nice thermal properties. Storage modulus is first more or less constant and then decreases. If the cross-linker content decreases, the storage modulus decreases as well but the shape of the curves looks different. The plateau of the beginning is not present, this is really seen in the 60:40 ratio (S4640). When particles are added (figure 3.15b), the same remark can be written: with a higher cross-linker content, the slope is less steep. From 50:50 ratio, the thermal properties are not that good.

The figure 3.15c represents the storage modulus of the high molecular weight diacrylate used in part II: the influence of the cross-linker leads to a shift of the curve in the direction of lower moduli.

3.4.3 Summary

To conclude this part, the content of cross-linker has to be chosen carefully: too much cross-linker and the polymer becomes very brittle although thermal properties are good. Not enough of it and elongation at break is very high but strength and thermal properties are not good. A balance between these two properties has to be found.

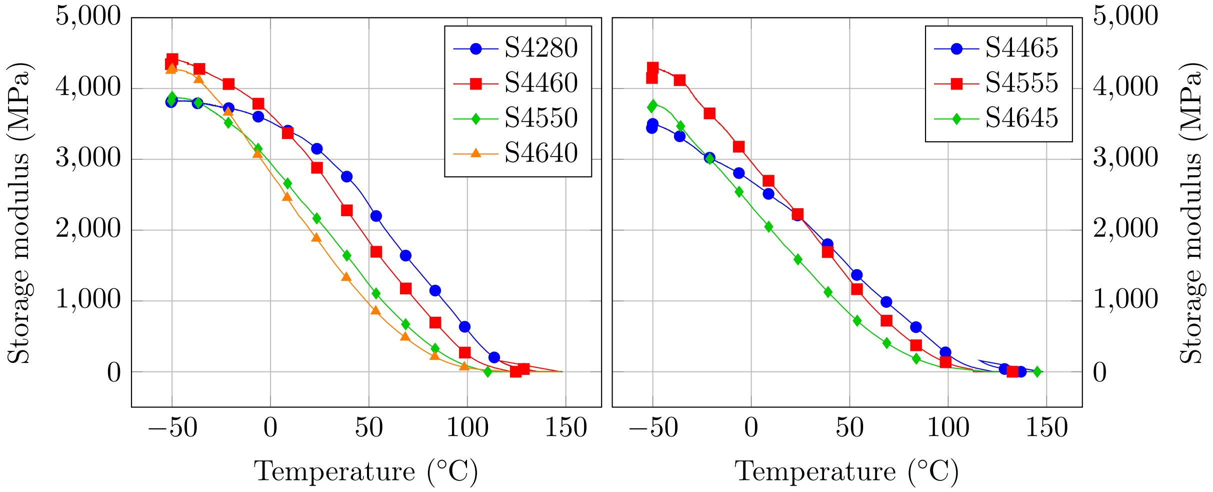

(a) S4xx0

(b) S4xx5

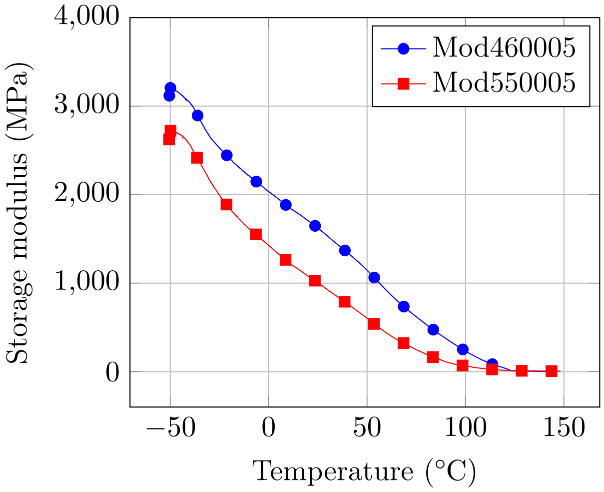

(c) Modxx0005

Figure 3.15 – Evolution of the storage modulus as function of the temperature with different amounts of cross-linker

Chapter 4

Conclusion

Additive manufacturing presents some advantages for the research of new materials. As technologies are fast and geometrically accurate, it is easy to test different kinds of polymers, to vary the composition of those polymers or to manufacture complex shapes.

Casting or injection moulding could also be used. Nevertheless, for highly viscous materials, casting might be a problem: indeed, if the viscosity is high, some air bubbles could remain in the material and thus its properties will not be optimal. Moreover, manufacturing the injection mould is expensive in comparison to drawing a 3D-model. If the design of the object has to be changed, injection moulding could become very expensive.

The last reason, and probably the most important one, why using additive manufacturing is the following: the final objects have a complex shape and they are difficult to manufacture with conventional technologies. Thus, it makes sense to use the same fabrication technique for the test samples. Figure 4.1 provides examples of objects manufactured in the lab.

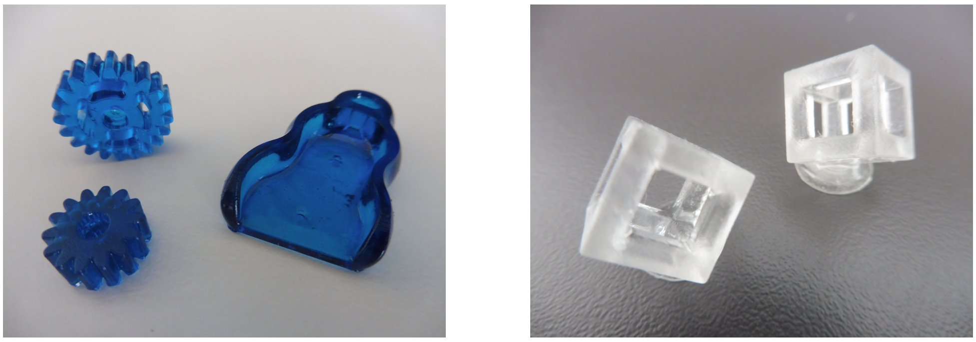

(a) Gear **(b)** Fancy cubes

Figure 4.1 – Examples of 3D-printed objects

In this master thesis, improvement of the mechanical properties of photopolymer resins is done by addition of impact modifiers, the core-shell particles. To figure out the useful properties of the experimental polymers, samples were manufactured with stereolithography and different tests were made:

- Viscosity measurements: information about temperature range for printing.
- Double bond conversion tests: information about the number of double bonds C=C which has reacted into single bonds C−C.

- Dynamic mechanic analysis (DMA): information about thermo-mechanical properties (T_g, storage modulus) and thermal stability of properties.
- Tensile tests (figure 4.2a): information about elongation at break and maximal strength. Seven samples were printed and the average value was calculated.
- Charpy impact tests (figure 4.2b): information about impact strength and cracks propagation. Nine samples were manufactured and the average value was also calculated.

(a) Tensile test **(b)** Charpy impact test

Figure 4.2 – Examples of tensile and Charpy impact tests

First, a commercial resin has been analysed to see the influence of these particles on the polymer properties: elongation at break and impact strength are enhanced with particles. Unfortunately, these particles decrease the thermal properties of the polymers. After the commercial resin, other formulations, combining a high molecular weight resin and a high T_g cross-linker, have been fabricated. The first compound should bring good elongation while the second one should change thermal properties. Although mechanical tests on these resins were better than those of the commercial one, the starting points (the properties of the polymer without particles) were quite low. It should be noted than less particles were needed to improve elongation as shown in figure 4.3 (9 wt% for the modified resin versus at least 16 wt% for the commercial resin).

Due to the low starting points, a search for better resins has been undertaken and two new formulations have been brought out. They have high elongation at break but poor thermal properties. The influence of the cross-linker has also been tested. The content of cross-linker in the formulation admits an optimum: indeed, if there is too much cross-linker, the material becomes highly brittle. In opposite, if there is not enough cross-linker, elongation at break will be high but thermal properties will be very bad.

A balance has to be found between good mechanical properties and thermal properties.

As core-shell particles improved in a good way the properties, two other factors, which could influence them, have been analysed: (1) decreasing the layer thickness of the samples was efficient and the properties were still improved. The major drawback of decreasing the layer thickness

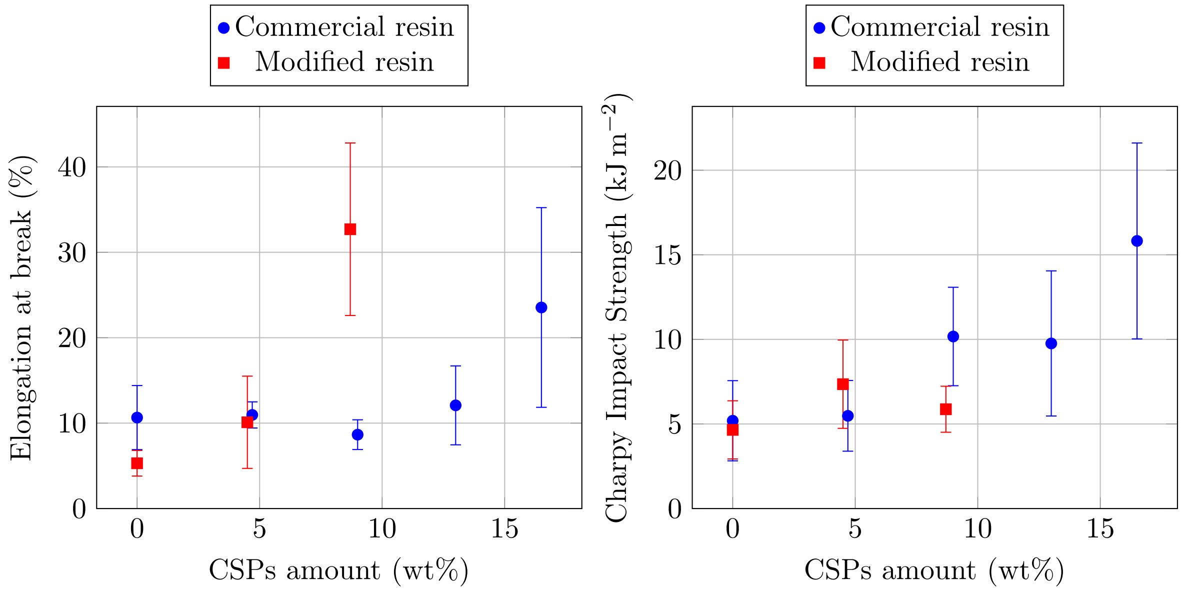

(a) Elongation at break **(b)** Charpy impact strength

Figure 4.3 – Comparison of the commercial resin and the modified resin (elongation at break and Charpy impact strength)

is the printing time. Indeed, if the layer thickness is divided by two,the printing time will be multiplied by two. (2) the scanning speed of the laser. However, the properties of the polymers were not really affected.

Some formulations gave good results in mechanical properties: mod550005 has 59.9 ± 9.9 % elongation at break and 57.2 ± 22.7 kJ m^{-2} Charpy impact strength. One of the Charpy probe did not break (sample 2 in figure 4.4). Formulation B555 has a high elongation at break (76.0 ± 15.2 %). Unfortunately, their thermal properties are not very good: at room temperature, their storage modulus is around 1000 MPa, which is quite low. Moreover, the slope of the storage modulus versus the temperature is high, which means that the mechanical properties strongly depend on the temperature.

As their elongation at break is high, these materials could be used for specific applications where the temperature does not change a lot and where good mechanical properties are asked.

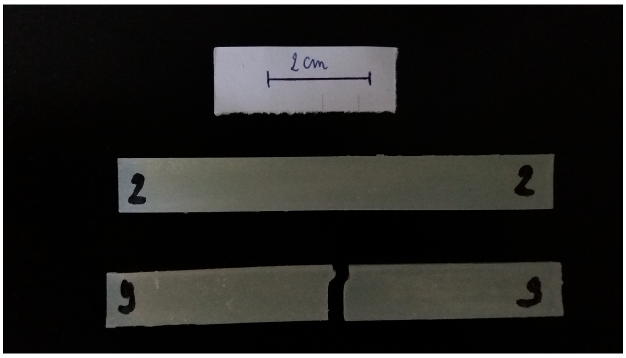

Figure 4.4 – Charpy impact test samples for Mod550005

To go further in this master thesis, here are some outlook which might be investigated:

- Add more cross-linker in the B55x material: B46x.
- Use another core-shell particle type.
- Use Polyphenylsulfone (PPSU) as impact modifier.
- Find a polymer with better initial thermal properties and improve it mechanically without reducing its thermal properties.

Appendix A

Formulations

Tables A.1 to A.3 give the weight percent of core-shell particles and the ratio between the resin and the cross-linker for every formulation used in this thesis.

Table A.1 – Formulations part I

Name	CSP content wt%CPS	Ratio	Comment
XR00	0.0	100:0	100 µm
XR05	4.5	100:0	100 µm
XR10	8.9	100:0	100 µm
XR15	12.9	100:0	100 µm
XR20	16.5	100:0	100 µm
XR00	0.0	100:0	50 µm
XR05	4.5	100:0	50 µm
XR10	8.9	100:0	50 µm
XR15	12.9	100:0	50 µm
XR20	16.5	100:0	50 µm

Table A.2 – Formulations part II

Name	CSP content wt%CPS	Ratio	Comment
Mod460000	0.0	40:60	medium speed
Mod460005	4.5	40:60	medium speed
Mod460010	8.7	40:60	medium speed
Mod460000	0.0	40:60	low speed
Mod460005	4.6	40:60	low speed
Mod460010	9.0	40:60	low speed
Mod550005	4.7	50:50	low speed
Mod370005	4.6	30:70	low speed

Table A.3 – Formulations part III

Name	CSP content wt%CPS	Ratio	Comment
S4640	0.0	60:40	50 µm
S4645	4.9	60:40	50 µm
S46410	9.0	60:40	50 µm
S4550	0.0	50:50	50 µm
S4555	4.8	50:50	50 µm
S45510	9.1	50:50	50 µm
S4460	0.0	40:60	50 µm
S4465	4.8	40:60	50 µm
S4280	0.0	20:80	50 µm
B550	0.0	50:50	50 µm
B555	4.7	50:50	50 µm
B5510	8.9	50:50	50 µm

Appendix B

Materials

The content of the formulations is secret and can not be disclosed.

B.1 Resins

B.2 Core-Shell Particles

B.3 Master Batch

Bibliography

[1] S. Wu, "Phase structure and adhesion in polymer blends: A criterion for rubber toughening," *Polymers*, vol. 26, pp. 1855–1863, 1985.

[2] ASTM F2792-12a, "Standard terminology for additive manufacturing technologies," 2013.

[3] I. Gibbson, D. W. Rosen, and B. Stucker, *Additive Manufacturing Technologies: Rapid Prototyping to Direct Digital Manufacturing.* Springer, 2010.

[4] A. Gebhardt, *Understanding Additive Manufacturing.* Hanser, 2011, ch. 2 Layer Manufacturing Processes, pp. 31–63.

[5] V. K. Wong and A. Hernandez, "A review of additive manufacturing," *ISRN Mechanical Engineering*, vol. 2012, 2012.

[6] http://www.custompartnet.com/wu/additive-fabrication, accessed: 2017-05-03.

[7] M. Kaur and A. K. Srivastava, "Photopolymerization: a review," *Journal of macromolecular science*, vol. C42, no. 4, pp. 481–512, 2002.

[8] V.-M. Archodoulaki and A. Ovsianikov, *Lecture Spezialkunststoffe [Polymers for special applications].* Vienna: TU Wien, 2016, ch. photopolymerization and photopolymers.

[9] R. W. Peiffer, "Applications of photopolymer technology," *ACS Symposium Series*, vol. 673, pp. 1–14, 1997.

[10] G. H. Michler and F. J. Baltá-Calleja, *Nano- and Micromechanics of Polymers.* Hanser, 2012, ch. 5 Fracture Phenomena and Mechanisms, pp. 159–182.

[11] A. S. Argon, R. E. Cohen, and T. M. Mower, "Mechanisms of toughening brittle polymers," *Materials Science and Engineering*, vol. A176, pp. 79–90, 1994.

[12] http://www.addmanu.at/fileadmin/shares/addmanu/docs/2015-leoben-stampfl_v2a.pdf, accessed: 2016-10-19.

[13] J. D. Moore, "Acrylonitrile-butadiene-styrene (ABS) - a review," *Composites*, vol. 4, no. 3, pp. 118–130, 1973.

[14] S. Olivera, H. B. Muralidhara, K. Venkatesh, K. Gopalakrishna, and C. S. Vivek, "Plating on acrylonitrile–butadiene–styrene (ABS) plastic: a review," *Journal of Materials Science*, vol. 51, no. 8, p. 3657–3674, 2016.

[15] https://www.sculpteo.com/en/glossary/abs-definition/, accessed: 2017-05-18.

[16] J. Brydson, "20 - polycarbonates," in *Plastics Materials (Seventh Edition).* Butterworth-Heinemann, 1999, pp. 556–583.

[17] http://www.resinex.fr/en/polymer-types/pc.html, accessed: 2017-05-19.

[18] http://www.plasticseurope.org/what-is-plastic/types-of-plastics-11148/engineering-plastics/pc.aspx, accessed: 2017-05-22.

[19] Solvay, "Radel® PPSU, veradel® PESU and acudel® modified PPSU - design guide," 2014.

[20] BASF, "Ultrason® E, S, P (PESU, PSU, PPSU) - product brochure," 2013.

[21] S. Göttgens and W. Sanner, "Polysulfone (PSU, PESU, PPSU)," *Kunststoffe Plast Europe*, vol. 95, no. 10, pp. 139–142, 2005.

[22] C. Maletzko and N. Herz, "Polyarylsulfone (PSU, PESU, PPSU)," *Kunststoffe International*, vol. 101, no. 10, pp. 90–96, 2011.

[23] S. Knaus and G. Allmaier, *Lecture Polymercharakterisierung [Polymer characterization].* Vienna: TU Wien, 2016.

[24] P. Burgholzer, T. Koch, E. Kozeschnik, C. Zaruba, J. Kastner, H. Riedl, and M. Bartosik, *Lecture Werkstoffcharakterisierung und zerstörungsfreie Prüfung [Materials Characterisation and Nondestructive Testing].* Vienna: TU Wien, 2015, chapter Thermal Analysis.